



Dimensional Analysis and Self-Similarity Theory for Regenerative Liquid Propellant Guns

by I. Kohlberg and T. P. Coffee

ARL-TR-2157

January 2000

Approved for public release; distribution is unlimited.

The findings in this report are not to be construed as an official Department of the Army position unless so designated by other authorized documents.

Citation of manufacturer's or trade names does not constitute an official endorsement or approval of the use thereof.

Destroy this report when it is no longer needed. Do not return it to the originator.

Army Research Laboratory

Aberdeen Proving Ground, MD 21005-5066

ARL-TR-2157

January 2000

Dimensional Analysis and Self-Similarity Theory for Regenerative Liquid Propellant Guns

I. Kohlberg

Kohlberg Associates, Inc.

T. P. Coffee

Weapons and Materials Research Directorate, ARL

Abstract

Regenerative liquid propellant guns (RLPGs) have been studied for many years. RLPG firings almost always show large, high-frequency pressure oscillations. To study this phenomenon, a fluid dynamics model of the combustion chamber/gun tube of an RLPG has been developed. High-frequency oscillations are generated naturally by the physics modeled in the code. Dimensional analysis has been applied to the governing equations to furnish insight into the dynamic relationships among pressure, density, temperature, droplet size, etc. The dimensional analysis predicts a scaling law between different-sized fixtures. The computational results exactly match these predictions. This agreement establishes the basis of self-similarity in the physical processes (e.g., tradeoff between droplet size and burning rate) and, in addition, helps verify the computational model.

Acknowledgments

The authors would like to thank John Knapton and Alexander Zielinski for their useful reviews of this report.

INTENTIONALLY LEFT BLANK.

Table of Contents

	<u>Page</u>
Acknowledgments.....	iii
List of Figures	vii
List of Tables	ix
1. Introduction	1
2. Dimensional Analysis Considerations	4
2.1 Basic Concepts	4
2.2 Review of Dimensional Analysis and Self-Similarity	5
2.3 Differential Equation Approach to Scaling of Burning Rate	8
3. Lumped Parameter Model for RLPG	19
3.1 Scaling of Differential Equations.....	19
3.2 Formal Dimensional Analysis Approach	27
3.3 Equivalence Between Approaches	32
4. Dimensionless Equations for a Test Fixture	35
4.1 Physical Model.....	35
4.2 Eulerian Equations	37
4.3 Self-Similar Eulerian Equations.....	41
4.4 Confirmation of Scaling Relationships	47
5. RLPG Considerations	53
6. Intact-Core Model	56
7. Conclusion.....	56
8. References	59
List of Symbols	61
Distribution List	65
Report Documentation Page	67

INTENTIONALLY LEFT BLANK.

List of Figures

<u>Figure</u>	<u>Page</u>
1. ARL 30-mm Concept VIC RLPG	2
2. In-Line Shower-Head RLPG.....	20
3. Sandia Test Fixture - Combustion Chamber	36
4. Sandia Test Fixture - Baseline: Simulation With 200- μ m-Diameter Droplets	49
5. Baseline FFT (Line) and All Physical Dimensions Doubled FFT (Dot)	50
6. Sandia Test Fixture - Simulation With Dimensions Doubled: 400- μ m-Diameter Droplets	51
7. Baseline-FFT (Line) and Doubled-FFT Frequency Times 2 (Dot).....	52
8. 30-mm Simulation - Pressure at Top Middle Wall	54
9. 60-mm Simulation - Pressure at Top Middle Wall	55

INTENTIONALLY LEFT BLANK.

List of Tables

<u>Table</u>	<u>Page</u>
1. Primary Set of Parameters and Variables.....	10
2. Additional Parameters and Variables Derived From the Primary Set	12
3. Variables, Parameters, and Dimensionality for the Shower-Head RLPG Model Described in Section 3.1.....	28

INTENTIONALLY LEFT BLANK.

1. Introduction

Pressure oscillations associated with combustion chamber instabilities in regenerative liquid propellant guns (RLPGs) have been studied for many years to attempt to identify sources of the instability and to develop techniques to mitigate the pressure excursions [1, 2]. Over the past year and a half, the U.S. Army Research Laboratory (ARL) has been exploring the use of "dimensional analysis theory" to simplify the description of RLPG combustion processes and to provide a firm theoretical foundation for research. Dimensional analysis theory can significantly reduce the number of key variables that need to be analyzed in order to efficiently search for ways for mitigating combustion chamber instabilities. This report summarizes the results of the study.

A diagram of the 30-mm concept VIC (6-C) RLPG is shown in Figure 1. The monopropellant in the liquid reservoir is prepressurized and located between the control piston and the injection piston. An igniter injects hot gas into the combustion chamber. As the chamber is pressurized, the control piston is pushed to the left, opening the injection orifice. The motion of the control piston depends on the balance of forces acting on the piston and includes the forces resulting from the pressure generated in the chamber, the retarding forces acting on the reservoir side of the piston, and the retarding forces associated with the damper assembly. The injection piston follows the control piston, injecting the propellant from the reservoir through the annular orifice. The combustion takes place in the combustion chamber, and the gas then flows into the gun tube. There is a large area change from the chamber to the tube.

Gun firings have been simulated using a lumped parameter code RLPGUN [3-6]. The injected liquid is assumed to instantaneously break up into droplets and ignite. The droplet diameter is obtained from an experimental correlation involving the entrance velocity, gas density, liquid density, etc. [7]. Although the functional form appears relevant, it is necessary to multiply the droplet diameter obtained from this correlation by a constant, which depends on the specific injection system, to obtain the proper pressure rise rate. This constant may depend on droplet coalescence; liquid in the intact core; a droplet ignition delay; or other simplifications in

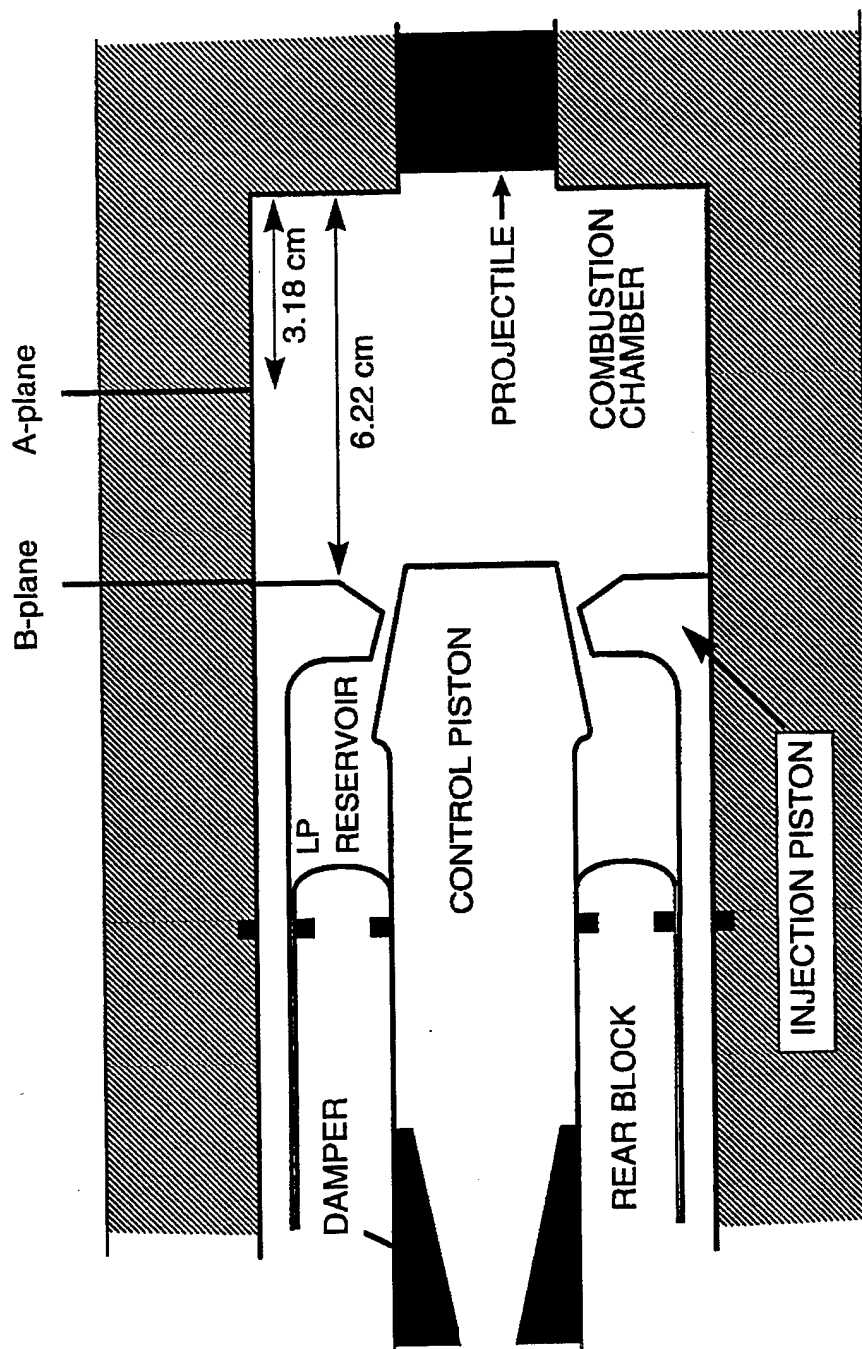


Figure 1. ARL 30-mm Concept VIC RLPG.

the breakup model, which do not fully represent the physical phenomena. The discrepancy could also be due to extrapolating data from low pressures in the experimental correlation to very high pressures with higher spray densities. However, using this modified correlation, good agreement with data taken in the tests has been obtained for a wide variety of RLPG firings.

Essentially, all firings of RLPGs show large-magnitude, high-frequency pressure oscillations that cannot be modeled using a lumped parameter code. To consider spatial variations, a two-dimensional/three-dimensional (2-D/3-D) model LPOSC has been written for the combustion chamber/gun tube of an RLPG [8, 9]. The piston motions, injection rate, and injected droplet size are all obtained from a lumped parameter code simulation. The propellant combustion rate is simulated based on an engineering correlation. Due to lack of information about spray behavior under gun conditions, the very simple breakup model and combustion rate equation from the lumped parameter code have also been used in LPOSC. Pressure waves are generated naturally by the model, and reasonable comparison with experimental data has been demonstrated.

Dimensional analysis is a mathematical tool that rigorously allows the most efficient way of establishing the minimal set of dimensionless functions that are required to analyze and interpret a physical problem such as the RLPG [10–13]. In addition, it permits the construction of experiments that are properly scaled. These scaled experiments can be used to efficiently organize and interpret the results of experiments and computer simulations that have already been performed. Additionally, they can be used to verify the internal consistency of mathematical models used in computer simulations [14].

We have taken the first several steps toward identifying the key parameter(s) responsible for combustion instabilities using the dimensional analysis approach. These findings have provided complementary insight that has been accrued by ARL and other organizations into the nature of combustion instabilities. For example, pressure oscillations do not scale between the 30-mm and 155-mm guns. Dimensional analysis provides insight into the physical reasons for the differences. As a natural consequence of our studies, we have also used the scaling aspect of

dimensional analysis theory to verify the mathematical correctness of gas and liquid transport developed in the ARL models.

2. Dimensional Analysis Considerations

2.1 Basic Concepts. Dimensional analysis has probably been used by nearly all scientists at one point or another in conjunction with simplifying a differential equation. Consider for example, the differential equation for the velocity, v ,

$$m \frac{dv}{dt} + \beta v^3 = 0, \quad (1)$$

with the initial condition, $v(t=0) = v_0$. The analytical solution of equation (1) is, of course trivial, but, if we could not solve it in closed form, we would write the solution as

$$v = v(m, \beta, v_0, t). \quad (2)$$

As observed, v appears to be a function of three parameters and time. Introducing the dimensionless velocity and time variables, $y = v/v_0$ and $\tau = \beta v_0^2 t/m$, respectively, reduces equation (2) to

$$\frac{dy}{d\tau} + y^3 = 0, \quad (3)$$

with initial condition, $y=1$. The universal solution of equation (3) is $y = y(\tau)$. A single solution describes the entire parameter space.

Comparison of equations (1) and (3) indicates the significant reduction in dimensionality that is possible by making appropriate substitutions to render the equations dimensionless. However,

is it possible to reduce dimensionality if we do not know the differential equations but do know the input parameters and variables? The answer is, “Yes,” and it is made possible by the classic work of Buckingham [10] that was developed in 1915. Buckingham showed how to reduce the number of parameters and variables; he called the reduced set “ Π -functions.”

The concepts of dimensional analysis are routinely used to improve our understanding of complex problems in the field of fluid mechanics and to organize the experimental data in the most efficient way (e.g., the use of Reynolds number). In some instances, the analytical form of the solution has been found from purely dimensional arguments (e.g., the blast wave equation [11]). A review of these formal methods is rendered in the next section.

We have explored the use of Buckingham’s theorem in selected subsets of the liquid rocket and RLPG problems (see sections 3.2 and 3.3). The approach generated too many Π -functions to be of any short-term use. We were, however, able to mathematically demonstrate the equivalence between this approach and the direct approach of working with the differential equations. Despite its lack of practical utility in this study, the formal theory may be useful in future investigations.

2.2 Review of Dimensional Analysis and Self-Similarity. The basis of Buckingham’s Π -theorem is summarized as follows. Assume a system can be described by “ n ” quantities, which can either be physical constants (e.g., universal gas constant), independent variables (e.g., time), or dependent variables (e.g., velocity, temperature), and “ m ” dimensions. The dimensions used in fluid mechanics that are relevant to our study are mass (M), length (L), time (T), and temperature (θ).

Now, let $u_1, u_2, u_3 \dots u_n$ denote the aforementioned n quantities. The solution of the problem yields a functional relationship of the form

$$F(u_1, u_2, u_3 \dots u_n) = 0. \quad (4)$$

If $\Pi_1, \Pi_2, \Pi_3 \dots$ etc., are dimensionless groupings of the u 's, Buckingham's theorem proves that a relationship of the form

$$f(\Pi_1, \Pi_2, \Pi_3 \dots \Pi_{n-m}) = 0 \quad (5)$$

can be derived. The dimensionality of the problem has, in principle, been reduced from n to $n - m$. The variables of the problem are the $n - m$ Π -functions. The reduction from n to $n - m$ variables can be very significant if n is not too large. For example, if $n = 6$ and $m = 4$, the problem is reduced to only two variables. In such cases, the solution may be accomplished analytically or by the solution of two differential equations. On the other hand, if $n = 15$ and $m = 4$, the number of variables is 11 and not much is gained.

Equation (5) represents $n - m$ equations in n unknowns. The solution of such a system is achieved using established matrix techniques of linear algebra and leads to $n - m$ relationships between the n unknowns. For tutorial, as well as practical purposes, we dispense with the matrix formalism and present the methodology based on the straightforward procedure developed by Streeter [13] for determining the Π 's.

- Step 1: Select m of the u 's, which collectively contain m of the dimensions. For example, if M , L , and T are the dimensions, we must select three of the u 's that collectively contain M , L , and T . Therefore $m = 3$ in this case.
- Step 2: Label the u 's in the manner consistent with step 1. Using $m = 3$ as an example, we select u_1, u_2 , and u_3 to be the three quantities that collectively contain the dimensions M , L , and T . We then label $u_4, u_5 \dots u_n$ as the remaining variables or parameters.
- Step 3: The $n - 3$ Π -functions are then constructed as follows:

$$\Pi_1 = u_1^{x_1} u_2^{y_1} u_3^{z_1} u_4$$

$$\Pi_2 = u_1^{x_2} u_2^{y_2} u_3^{z_2} u_5$$

.

.

.

$$\Pi_{n-3} = u_1^{x_{n-3}} u_2^{y_{n-3}} u_3^{z_{n-3}} u_n. \quad (6)$$

- Step 4: The final step in the method is to express the u 's in their dimensions and then determine the x 's, y 's, and z 's so that all the Π 's are dimensionless.

The aforementioned procedure is most readily explained by the example of a point explosion in air. This is the classic problem of a point explosion that has formed the foundation of many basic concepts of shock wave theory. An extensive treatise on the subject from the dimensional viewpoint can be found in Sedov's book [11]. It is presented here to show the recipe for constructing the dimensionless Π -functions.

For the point explosion in air, there are four variables: the radius of the shock wave, R ; the density of the ambient air, ρ ; the time after the explosion, t ; and the energy of the detonation, E . The dimensions of these quantities are

- R : L ,
- ρ : ML^{-3} ,
- t : T , and
- E : ML^2T^{-2} .

The selection of variables is

$$u_1 = R, u_2 = t, u_3 = \rho, \text{ and } u_4 = E. \quad (7)$$

Because there are only four variables, there is only one Π -function. It is determined by inserting equation (7) into equation (6) using the dimensionality of the variables. We have

$$\Pi_1 = R^x t^y \rho^z E = L^x T^y (M^z L^{-3z}) (ML^2 T^{-2}). \quad (8)$$

Setting the exponents of L, T, and M equal to 0 gives the following coupled set of equations:

$$x - 3z + 2 = 0, y - 2 = 0, \text{ and } z + 1 = 0. \quad (9)$$

The solution is $y = 2$, $z = -1$, and $x = -5$. Substituting the result into equation (8) then gives the dimensionless function

$$\Pi_1 = R^{-5} t^2 \rho^{-1} E. \quad (10)$$

In section 3.3, we construct sets of Π -functions for the lumped parameter model of the RLPG using the foregoing technique.

2.3 Differential Equation Approach to Scaling of Burning Rate. In section 2.1, we have shown how to construct a dimensionless differential equation from a dimensional equation by recognizing and using the inherent dimensionality of obvious physical quantities. This method is not only useful but is frequently the preferred method of constructing dimensionless equations that exhibit universal behavior. The major caveat in using this approach is that our mathematical model must be correct. If the physical description is not correctly described by the equations, erroneous scaling relations and predictions are possible.

The formal theory of dimensional analysis does not require a knowledge of the systems' differential or integral equations but only that we know what variables and parameters are involved. On the other hand, it provides insight into the relationship between the variables and parameters. Combined with a physical model of a system, dimensional analysis can provide guidance and proper scaling for experiments and simulations.

We call the method of constructing dimensionless equations from the original equations the "direct assault approach." The purpose of the analytical exercise of this section is to show how this method is used to explore the types of dimensionless variables that arise with the liquid propellant burning-rate expression. The reduction in the dimensionality of the problem and the ensuing scaling relationship are developed.

In this section, the combustion process is examined. A simplified model problem is considered. In this model, the volume, V , is constant. There are initially a specified number of droplets, all with the same diameter. The total mass in the system (gas plus liquid) is constant. The dynamic process is the conversion of the liquid into gas, releasing energy and increasing the pressure in the volume. The number of droplets remains constant as the droplets shrink in size.

Using the assumption that the total mass is constant, there is a relationship between the gas density and the droplet size. The burn rate is a function of the pressure. The process begins at $t = 0$. The initial conditions are the volume of the system, the diameter and number of droplets, and the density and temperature of the gas. The initial pressure is obtained from the Noble-Abel equation of state. In mathematical terms, the droplets are allowed to reach zero mass. This allows the total number of droplets to be conserved in the theoretical model.

The density is the average gas density per unit volume, that is, the gas mass divided by the volume. However, we must account for the fact that, when there are droplets within the volume, the actual gas density, ρ_G , will be much higher. We now calculate this increase. The 21 "primary" parameters and variables are defined in Table 1. What we mean by primary is that any other parameters and variables can be expressed in terms of this primary set.

Table 1. Primary Set of Parameters and Variables

Parameters/Variables	Definition
V	Volume
b	Covolume
p_0	Initial Gas Pressure
ρ_0	Initial Average Gas Density
p	Instantaneous Gas Pressure
ρ	Instantaneous Average Gas Density
N	Number of Droplets Contained in Volume, V (Remains Constant)
r_{D0}	Initial Radius of droplets
r_D	Instantaneous Radius of Droplets
R	Universal Gas Constant
T_G	Gas Temperature
T_{G0}	Initial Gas Temperature
e_L	Chemical Energy Per Unit Mass in Liquid
A	Burning-Rate Pre-Exponential
B	Burning-Rate Exponential
C_m	Specific Heat Per Unit Mass for Gas at Constant Volume
$C_p = C_m + R$	Specific Heat Per Unit Mass for Gas at Constant Pressure
$C_v = \rho_G C_m$	Specific Heat Per Unit Volume
$\gamma = \frac{C_p}{C_m}$	Ratio of Specific Heats
ρ_L	Intrinsic Density of Liquid
t	Time

Using the foregoing definitions, we have

$$C_p = \frac{\gamma}{\gamma - 1} R \quad (11)$$

and

$$C_m = \frac{R}{\gamma - 1}. \quad (12)$$

The internal energy per unit mass for the gas is

$$u = C_m T_G, \quad (13)$$

and the enthalpy per unit mass for the gas is

$$h = u + \frac{p}{\rho_G} = u + RT_G + pb = (C_m + R)T_G + pb = C_p + pb. \quad (14)$$

There are two equivalent forms for the equation of state:

$$p = \frac{\rho_G RT_G}{1 - b\rho_G} \quad (15a)$$

and

$$\rho_G = \frac{p}{RT_G + pb}. \quad (15b)$$

We must account for the fact that, when there are droplets within the volume, the actual gas density, ρ_G , will be much higher. In Table 2, we show the relationship between ρ and ρ_G with the help of additional parameters and variables that are derived from the primary set.

Table 2. Additional Parameters and Variables Derived From the Primary Set

Parameters/Variables	Definition
$n = \frac{N}{V}$	Number Density of Droplets (Remains Constant)
$v_D = \frac{4\pi}{3} r_D^3$	Instantaneous Volume of Droplet
$v_{D0} = \frac{4\pi}{3} r_{D0}^3$	Initial Volume of Droplet
$\eta_{D0} = n v_{D0}$	Initial Fraction of Volume Occupied by the Liquid
$1 - \eta_{D0}$	Initial Fraction of Volume Occupied by the Gas
$\eta_D = n v_D$	Instantaneous Fraction of Volume Occupied by the Liquid
$1 - \eta_D$	Instantaneous Fraction of Volume Occupied by the Gas
$\rho_{G0} = \frac{\rho_0}{1 - \eta_{D0}}$	Initial True Gas Density
$\rho_G = \frac{\rho}{1 - \eta_D}$	Instantaneous True Gas Density
$m_{D0} = \rho_L v_{D0}$	Initial Mass of Droplet
$m_D = \rho_L v_D$	Instantaneous Mass of Droplet
$M_{L0} = N m_{D0}$	Initial Total Mass of Liquid
$M_L = N m_D$	Instantaneous Total Mass of Liquid
$M_{G0} = \rho_{G0} (1 - \eta_{D0}) V$	Initial Mass of Gas
$M_G = \rho_G (1 - \eta_D) V$	Instantaneous Mass of Gas
$M = M_{L0} + M_{G0} = M_L + M_G$	Total Mass in System = Constant

The first step in the analysis is to establish the relationship between the dimensionless droplet size and the dimensionless true gas density. The starting point is the mass conservation equation:

$$M = M_{L0} + M_{G0} = M_L + M_G \quad (16)$$

and

$$N m_{D0} + \rho_{G0} (1 - \eta_{D0}) V = N m_D + \rho_G (1 - \eta_D) V. \quad (17)$$

Dividing by the volume, V , and making other substitutions gives

$$n\rho_L v_{D0} + \rho_{G0}(1 - nv_{D0}) = n\rho_L v_D + \rho_G(1 - nv_D). \quad (18)$$

We now introduce the following dimensionless variables

$$x = \frac{v_D}{v_{D0}} = \frac{r_D^3}{r_{D0}^3}, \quad (19)$$

$$y = \frac{\rho_G}{\rho_{G0}}, \quad (20)$$

and

$$g_0 = \frac{\rho_{G0}}{\rho_L}. \quad (21)$$

Equation (18) at first becomes

$$\eta_{D0}(1 - x) + g_0(1 - \eta_{D0}) = yg_0(1 - x\eta_{D0}), \quad (22)$$

which then gives

$$y = \frac{\eta_{D0}(1 - x) + g_0(1 - \eta_{D0})}{g_0(1 - x\eta_{D0})}. \quad (23)$$

Here, η_{D0} and g_0 are constants that depend only on the initial conditions. For brevity, we write

$$y = y(x, g_0, \eta_{D0}). \quad (24)$$

The burning-rate equation is

$$r_D = r_{D0} - A \int_0^t p^B(t') dt'. \quad (25)$$

Defining a dimensionless radius by the equation

$$\lambda = \frac{r_D}{r_{D0}} \quad (26)$$

and inserting the result into equation (25) gives

$$\lambda = 1 - \phi(t), \quad (27)$$

where

$$\phi(t) = \frac{A}{r_{D0}} \int_0^t p^B(t') dt'. \quad (28)$$

We then have

$$x = \frac{v_D}{v_{D0}} = \frac{r_D^3}{r_{D0}^3} = \lambda^3 \quad (29)$$

and

$$p^B(t) = \frac{r_{D0}}{A} \frac{d\phi}{dt} = -\frac{r_{D0}}{A} \frac{d\lambda}{dt}. \quad (30)$$

Using equation (15) applied for the initial conditions gives the following form of the dimensionless equation of state:

$$\frac{p}{p_0} = \frac{y(x, g_0, \eta_{D0})(1 - b\rho_{G0})}{1 - y(x, g_0, \eta_{D0})b\rho_{G0}} \left(\frac{T_G}{T_{G0}} \right) = \frac{y(x, g_0, \eta_{D0})(1 - \alpha_0)}{1 - y(x, g_0, \eta_{D0})\alpha_0} \left(\frac{T_G}{T_{G0}} \right), \quad (31)$$

where

$$\alpha_0 = b\rho_{G0}. \quad (32)$$

In order to define a dimensionless time and determine the dimensionless time dependence of the pressure and other quantities, it is necessary to express (T_G/T_{G0}) in terms of the dimensionless droplet radius. The required expression is now developed.

When volume of droplet changes from v_{D0} to v_D , the total amount of energy liberated by all the droplets is

$$E = e_L \rho_L N(v_{D0} - v_D) = e_L \rho_L N v_{D0} (1 - x). \quad (33)$$

where e_L is the propellant chemical energy per unit mass.

The temperature in the gas is computed from the equation

$$\Delta T_G = T_G - T_{G0} = \frac{E}{C_m M_G} = \frac{e_L \rho_L N v_{D0} (1 - x)}{C_m M_G}, \quad (34)$$

where E is given by equation (33) and the gas mass is given by

$$M_G = \rho_G (1 - \eta_D) V. \quad (35)$$

Using the equation

$$\eta_D = n v_D = n x v_{D0} = x \eta_{D0} \quad (36)$$

and the result of combining equations (20) and (23) gives

$$\begin{aligned} M_G &= \rho_{G0} \frac{\eta_{D0}(1-x) + g_0(1-\eta_{D0})}{g_0(1-x\eta_{D0})} (1-x\eta_{D0}) V \\ &= \rho_{G0} V \frac{\eta_{D0}(1-x) + g_0(1-\eta_{D0})}{g_0}. \end{aligned} \quad (37)$$

Inserting equation (37) into equation (34), using equation (21), and defining a new dimensionless quantity,

$$\beta_0 = \frac{e_L}{C_m T_0}, \quad (38)$$

then gives

$$\frac{T_G}{T_{G0}} = 1 + \frac{\beta_0 \eta_{D0}(1-x)}{(\eta_{D0}(1-x) + g_0(1-\eta_{D0}))} = 1 + K_T(\beta_0, \eta_{D0}, g_0, 1-x), \quad (39)$$

where

$$K_T = \frac{\beta_0 \eta_{D0}(1-x)}{(\eta_{D0}(1-x) + g_0(1-\eta_{D0}))}. \quad (40)$$

The first step in determining a time-dependent equation for the pressure is obtained by inserting equation (40) into equation (31). We have

$$\frac{p}{p_0} = \frac{y(x, g_0, \eta_{D0})(1 - \alpha_0)}{1 - y(x, g_0, \eta_{D0})\alpha_0} (1 + K_T(\beta_0, \eta_{D0}, g_0, 1 - x)). \quad (41)$$

Equation (41) shows that the time dependence of the pressure is determined by the time dependence of the dimensionless radius, $\lambda = x^{1/3}$; that is, $p(t)$ is an implicit function of time through the relationship $p(t) = p(\lambda(t))$. The other factors in equation (41), g_0, β_0, η_{D0} , and α_0 , are constants.

The explicit time dependence of the pressure is determined from equation (30). We write

$$\frac{d\lambda}{dt} = -\frac{Ap^B}{r_{D0}} = \frac{Ap_0^B}{r_{D0}} \frac{y^B(\lambda^3, g_0, \eta_{D0})(1 - \alpha_0)^B}{(1 - y(\lambda^3, g_0, \eta_{D0})\alpha_0)^B} (1 + K_T(\beta_0, \eta_{D0}, g_0, 1 - \lambda^3))^B. \quad (42)$$

Introducing the dimensionless time

$$\tau = \frac{t}{T_{D0}}, \quad (43)$$

where

$$T_{D0} = \frac{r_{D0}}{Ap_0^B}, \quad (44)$$

then gives the total dimensionless equation

$$\frac{d\lambda}{d\tau} = -F(\lambda, \tilde{\Omega}_0), \quad (45)$$

where

$$F(\lambda, \tilde{\Omega}_0) = \frac{y^B(\lambda^3, g_0, \eta_{D0})(1 - \alpha_0)^B}{(1 - y(\lambda^3, g_0, \eta_{D0})\alpha_0)^B} (1 + K_T(\beta_0, \eta_{D0}, g_0, 1 - \lambda^3))^B \quad (46)$$

and $\tilde{\Omega}_0$ is the set of dimensionless parameters: α_0, η_{D0}, g_0 , and β_0 .

The initial conditions are $\lambda = 1$ at $\tau = 0$. Because $F > 0$, λ will eventually go to 0 within a finite time, T_{end} . At this terminal time, all the droplets will have been converted to gas. T_{end} is determined by integrating equation (45) taken between the limits of $\lambda = 1$ to $\lambda = 0$:

$$T_{\text{end}} = \int_0^1 \frac{d\lambda'}{F(\lambda', \tilde{\Omega}_0)} \quad (47)$$

Once $\lambda(\tau)$ is obtained, we determine $p(\tau)$ from equation (30) and (41).

$$p^B(\tau) = -\frac{r_{D0}}{A} \frac{d\lambda}{dt} = -\frac{r_{D0}}{A} \frac{d\lambda}{d\tau} \frac{d\tau}{dt} = p_0^B F(\lambda(\tau), \tilde{\Omega}_0) \quad (48)$$

and

$$\frac{p(\tau)}{p_0} = \frac{y(\lambda^3, g_0, \eta_{D0})(1 - \alpha_0)}{(1 - y(\lambda^3, g_0, \eta_{D0})\alpha_0)} (1 + K_T(\beta_0, \eta_{D0}, g_0, 1 - \lambda^3)). \quad (49)$$

In summary, the use of dimensional analysis, combined with specific knowledge of the differential equations that define the system, has reduced the solution of a complicated burning-rate problem to the evaluation of a single integral. Only the following four dimensionless parameters, that is,

$$\eta_{D0} = n v_{D0}, \quad g_0 = \frac{\rho_{G0}}{\rho_L}, \quad \alpha_0 = b \rho_{G0}, \quad \text{and} \quad \beta_0 = \frac{e_L}{C_m T_0},$$

are required to distinguish one solution from another. Originally, 21 parameters were used to set up the problem.

3. Lumped Parameter Model for RLPG

3.1 Scaling of Differential Equations. The purpose of this section is to use the direct assault technique of dimensional analysis theory in order to gain some insight into how dimensionless parameters might be useful for understanding pressure oscillations caused by combustion pressure instabilities. The model we have selected here is a simplification of the lumped parameter RLPG configuration originally developed by Coffee [3]. This model is physically and mathematically not capable of representing pressure oscillations. Its primary use in this study is to obtain a preliminary assessment of the potential gains in simplification using dimensional analysis theory. Pressure oscillations are considered in section 4.

The basic notion was that, if dimensional analysis was not useful in predicting scaling relationships in this major simplification of an RLPG system, it was not likely to work in a more realistic model. Fortunately, scaling relationships derived for this model were confirmed by numerical analyses using the ARL code. These test cases are presented at the end of this section.

We show that a combination of analytical techniques, combined with the direct assault on the resulting equations, is very useful. The mathematical foundation for the study of pressure oscillations makes three simplifications to Coffee's model: the piston is weightless, the liquid propellant is incompressible, and the projectile is motionless. The first two assumptions were found quite acceptable using numerical evaluations of previous studies. The third assumption is equivalent to assuming an infinitely heavy projectile.

The physical model is similar to that shown in Figure 2, an in-line shower-head RLPG [3]. In this diagram, A_1 is the area of the piston on the liquid side, A_3 is the area of the piston on the chamber side, and A_v is the area of the vents that permit propellant to flow from its reservoir

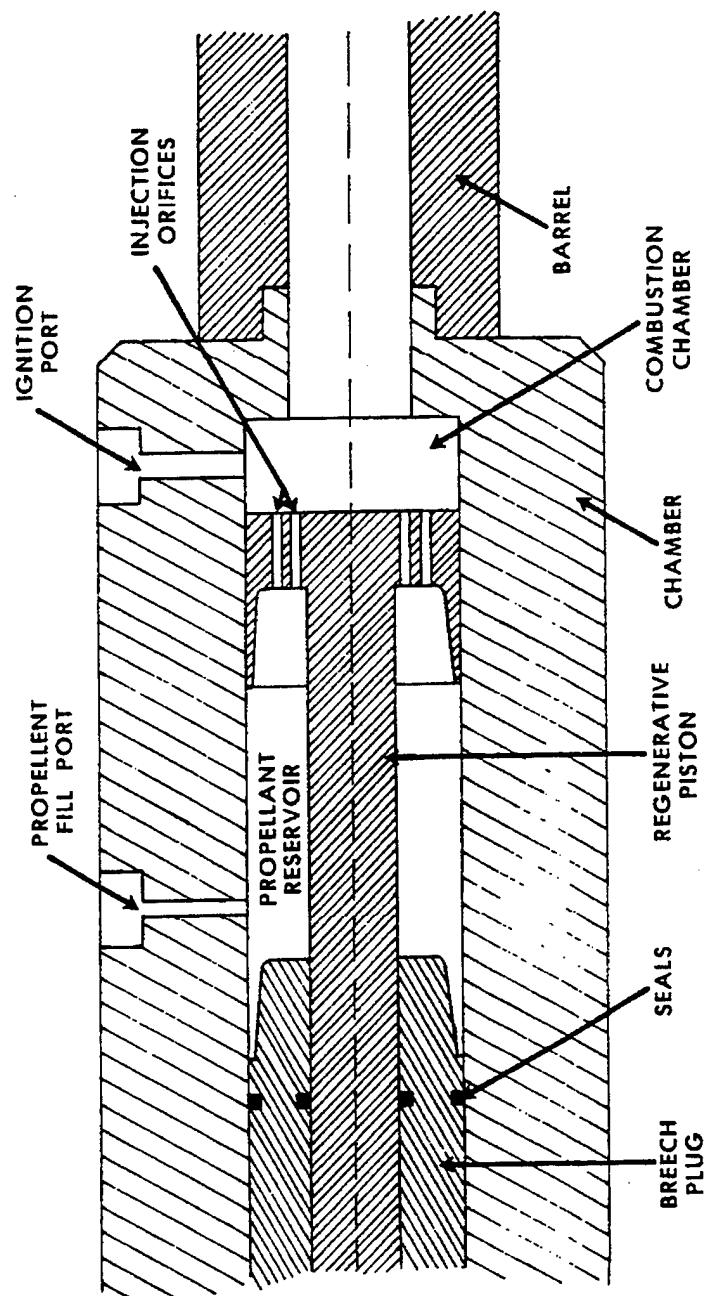


Figure 2. In-Line Shower-Head RLPG.

into the combustion chamber. V_3 is the time-dependent volume of the combustion chamber, and V_1 is the time-dependent volume of the propellant reservoir.

Coffee [3] has developed a complete set of equations that describes the system in the absence of the three simplifications made here. We do not duplicate his analysis in detail. We do, however, include a limited number of equations that have led us to the final result.

The net result of our analysis is the development of the dimensionless differential equations, equations (72) and (73). These equations allow us to make scaling predictions that include time behavior based on dimensional analysis.

As the pressure in the chamber increases, the piston is pushed to the left. If V_{10} is the initial volume of the liquid propellant chamber, the volume, V_1 , at time t is given by

$$V_1 = V_{10} - S_{ps}A_1. \quad (50)$$

S_{ps} is the displacement from the initial condition, measured positive when moving to the left. It is related to the piston velocity, v_{ps} , via the equation

$$\frac{dS_{ps}}{dt} = v_{ps}; \quad (51)$$

v_{ps} is also positive when the motion is to the left.

When the piston is weightless, there is no net force on the piston. The liquid and gas forces on the piston must be balanced, giving the equation

$$p_3 (A_3 - A_v) = p_1 (A_1 - A_v). \quad (52)$$

Here, p_3 is the gas pressure in the chamber and p_1 is the liquid pressure in the reservoir. Liquid enters the chamber from the reservoir through the vents. Equation (52) immediately provides the relationship between the differential pressure and the pressure in the combustion chamber. We have

$$p_1 - p_3 = \eta p_3, \quad (53)$$

where

$$\eta = \frac{A_3 - A_1}{A_1 - A_v}. \quad (54)$$

Since $A_3 - A_v > A_1 - A_v$, the pressure in the reservoir is greater than that of the chamber and liquid will flow into the chamber.

The time dependence of the mass flow rate, \dot{m} , into the chamber is controlled only by the time dependence of p_3 . This is easily shown starting with the equation

$$\dot{m} = C_d \rho_L A_v v_3, \quad (55)$$

where C_d is the discharge coefficient and v_3 is the velocity of the liquid as it enters the chamber. The specific value of C_d is inconsequential for our analysis, and, for this reason, it is set equal to 1.0. Equation (55) then becomes

$$\dot{m} = \rho_L A_v v_3, \quad (56)$$

where v_3 is determined from Bernoulli's law for streamline flow. The general expression is

$$v_3^2 = v_1^2 + \frac{2(p_1 - p_3)}{\rho_L}. \quad (57)$$

Assuming that $v_1 = 0$ and inserting the resulting expression into equation (56) gives

$$\dot{m} = A_v \sqrt{2\rho_L (p_1 - p_3)} = A_v \sqrt{2\rho_L \eta p_3} = \psi \sqrt{p_3}, \quad (58)$$

where

$$\psi = A_v \sqrt{2\rho_L \eta}. \quad (59)$$

Using equation (58) in combination with the assumption of incompressibility of the liquid enables us to relate the mass flow rate to the velocity of the piston. The decrease in volume of the reservoir is

$$\frac{dV_1}{dt} = -v_{ps} A_1. \quad (60)$$

With $v_{ps} A_1 \rho_L$ as the mass loss in the reservoir per unit time, it must equal the mass flow rate into the chamber. This gives

$$v_{ps} A_1 = A_v v_3. \quad (61)$$

The temporal relationship between the mass density, ρ_3 , and volume, V_3 , within the chamber is derived in terms of the initial conditions from equations (58) to (61). The increase in chamber volume is given by

$$\frac{dV_3}{dt} = v_{ps} A_3 = \xi \sqrt{p_3}, \quad (62)$$

where

$$\xi = \frac{A_3 A_v}{A_1} \sqrt{\frac{2\eta}{\rho_L}}. \quad (63)$$

The increase in total mass (equation [58]) of gas in the chamber, M_3 , is given by

$$\frac{dM_3}{dt} = \dot{m} = \psi \sqrt{p_3}. \quad (64)$$

From equations (62) and (64), we obtain

$$\frac{dV_3}{dM_3} = \frac{\alpha}{\rho_L}, \quad (65)$$

where

$$\alpha = \frac{A_3}{A_1} > 1. \quad (66)$$

Integrating equation (65) between the initial conditions (denoted by the additional subscript "0") and the state at a later time gives

$$V_3 = V_{30} \frac{\left(1 - \frac{\alpha \rho_{30}}{\rho_L}\right)}{\left(1 - \frac{\alpha \rho_3}{\rho_L}\right)}. \quad (67)$$

Using equation (67) in conjunction with the Noble-Abel equation of state,

$$p_3 = \frac{(\gamma - 1)\rho_3 C_v T_3}{(1 - b\rho_3)}, \quad (68)$$

and the energy balance equation derived by Coffee [3],

$$\rho_3 C_p \frac{dT_3}{dt} = - \left(\frac{\partial \ln \rho_3}{\partial \ln T_3} \right)_{p_3} \dot{m} \left(e_L + \frac{(1 + \eta)p_3}{\rho_L} - C_p T_3 - b p_3 \right) + \frac{\dot{m}}{V_3}, \quad (69)$$

reduces the solution of the problem to two simultaneous time-dependent equations for the pressure and density. The details are tedious but straightforward. From these two equations, we can derive two equivalent dimensionless equations. The variables in these dimensionless equations are the dimensionless density, $\hat{\rho}$, and the dimensionless pressure, \hat{p} . For this transient problem, it is convenient to define

$$\hat{\rho}_3 = \frac{\rho_3}{\rho_{30}}, \quad (70)$$

and

$$\hat{p}_3 = \frac{p_3}{p_{30}}. \quad (71)$$

The derived time-dependent equations are

$$\frac{d\hat{\rho}_3}{dt} = \frac{(1 - \beta \hat{p}_3)^2}{(1 - \beta)} \sqrt{\hat{p}_3} \quad (72)$$

and

$$\frac{d\hat{p}_3}{d\hat{t}} = \frac{\gamma\hat{p}_3}{\hat{p}_3(1-k\hat{p}_3)} \frac{d\hat{p}_3}{d\hat{t}} + \frac{(1-\beta\hat{p}_3)(\gamma-1)(\hat{h}_1-\hat{h}_3)\sqrt{\hat{p}_3}}{(1-\beta)(1-k\hat{p}_3)}. \quad (73)$$

Here, \hat{t} is a dimensionless time and is defined by the equation

$$\hat{t} = \frac{t}{\tau}, \quad (74)$$

where τ is a characteristic time constant for the system; it is defined by the equation

$$\frac{1}{\tau} = \sqrt{\frac{p_{30}\rho_L}{\rho_{30}^2}} \frac{(\sqrt{2\eta})A_v}{V_{30}}. \quad (75)$$

All the variables and parameters in equations (72) and (73) are dimensionless. They are

- $\hat{h}_1 = \hat{e}_1 + g\hat{p}_3,$

- $\hat{h}_3 = \frac{\hat{p}_3(\gamma - k\hat{p}_3)}{\hat{p}_3(\gamma - 1)},$

- $\hat{e}_1 = \frac{e_L}{c_{30}^2},$

- $g = \frac{\rho_{30}}{\rho_L}(1 + \eta),$

- $\eta = \frac{A_3 - A_1}{A_1 - A_v} = \frac{\frac{A_3}{A_1} - 1}{1 - \frac{A_v}{A_1}},$

- $k = b\rho_{30},$ and

- $\beta = \frac{A_3}{A_1} \frac{\rho_{30}}{\rho_L}$, where

- $c_{30}^2 = \frac{p_{30}}{\rho_{30}}$.

A close examination of equation (73) and the associated definition shows that the time behavior for the dimensionless pressure and density as a function of dimensionless time are function of only five dimensionless parameters. These parameters form the set, Ω , where

$$\Omega = \{b\rho_{30}, \frac{A_3}{A_1}, \frac{\rho_{30}}{\rho_1}, \frac{A_v}{A_1}, \frac{e_1}{c_{30}^2}\}. \quad (76)$$

Systems that have the same values of the five dimensionless constants in equation (76) will exhibit identical time behavior as a function of dimensionless time, \hat{t} . If systems have the same values of equation (76) but differ in the characteristic time constant, τ , their motion in real time will be self-similar or, simply, similar; that is, the motion will look identical but in different time scales.

We have numerically confirmed the self-similarity predictions of equations (72) and (73) for a variety of test cases using the ARL computer model. The success of this analysis paved the way for the study of the more sophisticated Sandia National Laboratories (SNL) test fixture discussed in section 4.

3.2 Formal Dimensional Analysis Approach. Table 3 lists the variables, parameters, and dimensionality for the model described in section 3.1. For convenience in constructing the Π -functions, we have divided the variables in classes that contain the same dimensions. It is of interest to see how the formal theory of dimensional analysis, based on Buckingham's

Table 3. Variables, Parameters, and Dimensionality for the Shower-Head RLPG Model Described in Section 3.1

Symbol	Definition	Dimensions	Index	Class
Time				
t	Time	T	u ₁	Basis
Areas				
A ₁	Piston Area on Liquid Side	L ²	u ₂	Basis
A ₃	Piston Area on Combustion Side	L ²	u ₅	1
A _v	Vent Area	L ²	u ₆	1
Volumes				
V ₃₀	Initial Volume of Chamber	L ³	u ₇	2
V ₃	Instantaneous Volume of Chamber	L ³	u ₈	2
Density Related				
ρ ₁	Liquid Density	ML ⁻³	u ₉	3
ρ ₃₀	Initial Gas Density	ML ⁻³	u ₁₀	3
ρ ₃	Instantaneous Gas Density	ML ⁻³	u ₁₁	3
b	Covolume	M ⁻¹ L ³	u ₃	Basis
Pressures				
p ₁	Fluid Pressure	ML ⁻¹ T ⁻²	u ₁₂	4
p ₃₀	Instantaneous Pressure in Chamber	ML ⁻¹ T ⁻²	u ₁₃	4
p ₃	Initial Pressure in Chamber	ML ⁻¹ T ⁻²	u ₁₄	4
Velocities				
v ₃	Propellant Velocity Into Chamber	LT ⁻¹	u ₁₅	5
v _{ps}	Piston Velocity	LT ⁻¹	u ₁₆	5
Energetics				
C _p	Specific Heat at Constant Pressure	L ² T ⁻² θ ⁻¹	u ₁₇	6
θ _c	Chamber Temperature	θ	u ₄	Basis
e _L	Propellant Energy Per Unit Mass	L ² T ⁻²	u ₁₈	7

Π -theorem, determines the dimensionless variables. In the next section, we show the equivalence between the two methods.

For a system involving “m” dimensions and a total of “n” variables, the Π -functions are labeled and constructed according to the following scheme:

$$\Pi_{n-m} = u_1^{w_{n-m}} u_2^{x_{n-m}} u_3^{y_{n-m}} u_4^{z_{n-m}} u_n; \quad n > m. \quad (77)$$

By expressing the u_n in terms of their dimensions, we determine the Π_{n-m} by requiring the product of equation (77) to be nondimensional. Those u_n that have the same dimensions will have the same values of w_{n-m} , x_{n-m} , y_{n-m} , and z_{n-m} .

In our case, there are $m =$ four dimensions, M, L, T, and θ , and a total of $n = 18$ variables/parameters. There will then be $18 - 4 = 14$ Π -functions. The basis functions are

- $u_1 = t$,
- $u_2 = A_1$,
- $u_3 = b$, and
- $u_4 = \theta_c$.

Working through the procedure developed in section 2.2, we determine the 14 Π -functions.

- Class 1:

$$(1) \quad \Pi_1 = t^{w_1} A_1^{x_1} b^{y_1} \theta_c^{z_1} A_3 = T^{w_1} L^{2x_1} M^{-y_1} L^{-3y_1} \theta^{z_1} L^2 = \frac{A_3}{A_1} \text{ and}$$

$$(2) \quad \Pi_2 = t^{w_1} A_1^{x_1} b^{y_1} \theta_c^{z_1} A_v = T^{w_2} L^{2x_2} M^{-y_2} L^{-3y_2} \theta^{z_2} L^2 = \frac{A_v}{A_1}, \text{ where}$$

$$w_1 = w_2 = 0; x_1 = x_2 = -1; y_1 = y_2 = 0; z_1 = z_2 = 0.$$

• Class 2:

$$(3) \quad \Pi_3 = t^{w_3} A_1^{x_3} b^{y_3} \theta_c^{z_3} V_{30} = T^{w_3} L^{2x_3} M^{-y_3} L^{-3y_3} \theta^{z_3} L^3 = \frac{V_{30}}{A_1^{3/2}} \text{ and}$$

$$(4) \quad \Pi_4 = t^{w_4} A_1^{x_4} b^{y_4} \theta_c^{z_4} V_3 = T^{w_4} L^{2x_4} M^{-y_4} L^{3y_4} \theta^{z_4} L^3 = \frac{V_3}{A_1^{3/2}}, \text{ where}$$

$$w_3 = w_4 = 0; x_3 = x_4 = -3/2; y_3 = y_4 = 0; z_3 = z_4 = 0.$$

Following the same procedure, we state the results for the remaining Π -functions in simpler form by deleting references to the values for w , x , y , and z .

• Class 3

$$(5) \quad \Pi_5 = t^w A_1^x b^y \theta_c^z P_L = T^w L^{2x} M^{-y} L^{3y} \theta^z M L^{-3} = b\rho_L,$$

$$(6) \quad \Pi_6 = t^w A_1^x b^y \theta_c^z \rho_{30} = T^w L^{2x} M^{-y} L^{3y} \theta^z M L^{-3} = b\rho_{30}, \text{ and}$$

$$(7) \quad \Pi_7 = t^w A_1^x b^y \theta_c^z \rho_3 = T^w L^{2x} M^{-y} L^{3y} \theta^z M L^{-3} = b\rho_3.$$

• Class 4:

$$(8) \quad \Pi_8 = t^w A_1^x b^y \theta_c^z p_1 = T^w L^{2x} M^{-y} L^{3y} \theta^z M L^{-1} T^{-2} = t^2 A_1^{-1} b p_1,$$

$$(9) \quad \Pi_9 = t^w A_1^x b^y \theta_c^z p_{30} = T^w L^{2x} M^{-y} L^{3y} \theta^z M L^{-1} T^{-2} = t^2 A_1^{-1} b p_{30}, \text{ and}$$

$$(10) \quad \Pi_{10} = t^w A_1^x b^y \theta_c^z p_3 = T^w L^{2x} M^{-y} L^{3y} \theta^z M L^{-1} T^{-2} = t^2 A_1^{-1} b p_3.$$

• Class 5:

$$(11) \Pi_{11} = t^w A_1^x b^y \theta_c^z v_3 = T^w L^{2x} M^{-y} L^{3y} \theta^z L T^{-1} = t A_1^{-1/2} v_3 \text{ and}$$

$$(12) \Pi_{12} = t^w A_1^x b^y \theta_c^z v_{ps} = T^w L^{2x} M^{-y} L^{3y} \theta^z L T^{-1} = t A_1^{-1/2} v_{ps}.$$

• Class 6:

$$(13) \Pi_{13} = t^w A_1^x b^y \theta_c^z C_p = T^w L^{2x} M^{-y} L^{3y} \theta^z L^2 T^{-2} \theta^{-1} = t^2 A_1^{-1} \theta_c C_p.$$

• Class 7:

$$(14) \Pi_{14} = t^w A_1^x b^y \theta_c^z e_L = T^w L^{2x} M^{-y} L^{3y} \theta^z L^4 T^{-4} = t^2 A_1^{-1} e_L.$$

The general solution to problem is given by

$$F(\Pi_1, \Pi_2, \dots, \Pi_{13}, \Pi_{14}) = 0. \quad (78)$$

Because of the large number of Π -functions and their cumbersome forms, equation (78) is not especially useful. It is necessary to reduce both the number and complexity of the Π -functions. We now discuss methods for accomplishing this.

It will be recalled that, in the direct assault approach of the previous section, we ended up with two ordinary time dependent differential equations for the dimensionless pressure, $\hat{p}_3 = p_3 / p_{30}$, and the dimensionless density, $\hat{\rho}_3 = \rho_3 / \rho_{30}$. Without even solving equations (72) and (73) of the previous section, we can write their solutions in the forms

$$\hat{\rho}_3 = \Psi_p\left(\frac{t}{\tau}, b\rho_{30}, \frac{A_3}{A_1}, \frac{\rho_{30}}{\rho_1}, \frac{A_v}{A_1}, \frac{e_L}{c_{30}^2}\right) \quad (79)$$

and

$$\hat{p}_3 = \Psi_p \left(\frac{t}{\tau}, b\rho_{30}, \frac{A_3}{A_1}, \frac{\rho_{30}}{\rho_1}, \frac{A_v}{A_1}, \frac{e_L}{c_{30}^2} \right), \quad (80)$$

with Ψ_p and Ψ_p as functions of their respective arguments.

It is recalled that equations (72) and (73) are two coupled equations. It is possible to solve these equations in quadrature by initially formulating the single differential equation:

$$\frac{d\hat{p}_3}{d\hat{p}_3} = f(\hat{p}_3, \hat{p}_3, \Omega). \quad (81)$$

The result of the foregoing discussion is that the solution of equations (72) and (73) can be expressed in the form

$$F'(\hat{p}_3, \hat{p}_3, b\rho_{30}, \frac{A_3}{A_1}, \frac{\rho_{30}}{\rho_1}, \frac{A_v}{A_1}, \frac{e_L}{c_{30}^2}) = 0, \quad (82)$$

where F' is a function of the seven variables of equation (82).

By comparing equations (78) and (82), we immediately see that the former set contains twice the number of variables than the latter. This condition resulted by solving some of the algebraic equations in the system. That is, we were able to eliminate some of the variables altogether (e.g., temperature, piston velocity, etc.) by expressing them in terms of other variables. It is apparent that, if we are able to formulate all the equations to begin with, as we can in this simple problem, there is probably no need, or very limited need, for using formal dimensional analysis.

3.3 Equivalence Between Approaches. It is of interest to compare equation (82) with the 14 Π -functions previously generated. For this, we need to recall that the Π -functions are members of a group, and satisfy the following group properties.

- If Π_i is a member of the group, so is Π_i^n , where n is any positive or negative real number.
- If Π_i and Π_j are members of the group so is $\Pi_i^n \Pi_j^m$, where n and m are any positive or negative real numbers.

Thus, there is nothing unique about the 14 previously generated Π -functions. Using the two group properties just listed, a completely different set of Π -functions can be constructed, which is better suited to physical interpretation. For example, the pervasive appearance of time, t , in so many of the Π -functions does not enhance one's physical insight into the nature of the solution. The dependence of so many of the Π -functions on t is easily rectified using the group properties.

For now, all we want to do is to show how equation (82) can be expressed in terms of a modified subset of the 14 original Π -functions using the group properties. The first few steps are easy to see:

$$\hat{p}_3 = \frac{p_3}{p_{30}} = \frac{\Pi_{10}}{\Pi_9}, \quad (83)$$

$$\frac{A_3}{A_1} = \Pi_1, \quad (84)$$

$$\frac{A_v}{A_1} = \Pi_2, \quad (85)$$

$$bp_{30} = \Pi_6, \quad (86)$$

$$\frac{\rho_{30}}{\rho_1} = \frac{\Pi_6}{\Pi_5}, \quad (87)$$

and

$$\hat{\rho}_3 = \frac{\rho_3}{\rho_{30}} = \frac{\Pi_7}{\Pi_6}. \quad (88)$$

Now, consider the term e_L / c_{30}^2 . We express c_{30}^2 as follows:

$$c_{30}^2 = \frac{\rho_{30}}{\rho_{30}} = \frac{\Pi_9}{t^2 A_1^{-1} \Pi_6}. \quad (89)$$

Dividing Π_{14} by $(\Pi^*)^2$ gives

$$\frac{e_L}{c_{30}^2} = \frac{\Pi_{14} \Pi_6}{\Pi_9}. \quad (90)$$

Since there is nothing unique about any of the Π_i , the ratios of Π -functions depicted in equations (87) to (90) are just as valid as the original set of Π -functions. We now define a new set of Π -functions (using a "bar" over the Π symbol) in terms of the initial set:

$$\begin{aligned} \bar{\Pi}_1 &= \Pi_1, & \bar{\Pi}_2 &= \Pi_2, & \bar{\Pi}_3 &= \Pi_3, & \bar{\Pi}_4 &= \Pi_4, & \bar{\Pi}_5 &= \frac{\Pi_6}{\Pi_5}, \\ \bar{\Pi}_6 &= \Pi_6, & \bar{\Pi}_7 &= \frac{\Pi_7}{\Pi_6}, & \bar{\Pi}_8 &= \Pi_8, & \bar{\Pi}_9 &= \Pi_9, & \bar{\Pi}_{10} &= \frac{\Pi_{10}}{\Pi_9}, \\ \bar{\Pi}_{11} &= \Pi_{11}, & \bar{\Pi}_{12} &= \Pi_{12}, & \bar{\Pi}_{13} &= \Pi_{13}, & \bar{\Pi}_{14} &= \frac{\Pi_{14} \Pi_6}{\Pi_9}. \end{aligned} \quad (91)$$

Equation (82) now becomes

$$F(\bar{\Pi}_1, \bar{\Pi}_2, \bar{\Pi}_5, \bar{\Pi}_6, \bar{\Pi}_7, \bar{\Pi}_{10}, \bar{\Pi}_{14}) = 0. \quad (92)$$

The foregoing equation or its equivalent, equation (82), is actually easier to use than it would appear. The reason for this is that some of the $\bar{\Pi}$ -functions are actually constants, or parameters that do not change much. For example, $\bar{\Pi}_5$ and $\bar{\Pi}_6$ are expected to be nearly constant under most conditions. If the combustion chamber is designed to retain constant area ratios, then $\bar{\Pi}_1$ and $\bar{\Pi}_2$ are constants and equation (82) becomes

$$F(\hat{p}_3, \hat{p}_3, \frac{e_L}{c_{30}^2}) = 0. \quad (93)$$

Equation (93) shows that, under the aforementioned conditions, the relationship between pressure and density depends only on the single dimensionless variable, e_L / c_{30}^2 . The time scale associated with the behavior of pressure and density is determined from equations (72) and (73).

For systems where there is high confidence that the physics have been accurately modeled, the direct assault approach is probably the best method for determining the significant dimensionless variables. On the other hand, when the equations that describe the system are not well defined, the formal theory can provide guidance in deducing significant dimensionless parameters. The virtue of being able to solve a portion of the problem is the reduction of the number of Π -functions.

4. Dimensional Analysis for a Test Fixture

4.1 Physical Model. A simplified problem has been chosen. A test fixture, Figure 3, was developed at SNL to study pressure oscillations [15]. The combustion chamber in the fixture is basically a cylinder with a 1-in radius. Liquid propellant is injected through a circular opening on the center line at the left of the chamber by a differential piston. Hot gas, and possibly some liquid, flow through a converging orifice at the right into atmospheric pressure. Pressure oscillations are quickly established in the chamber. Normally, there is a single, clear frequency

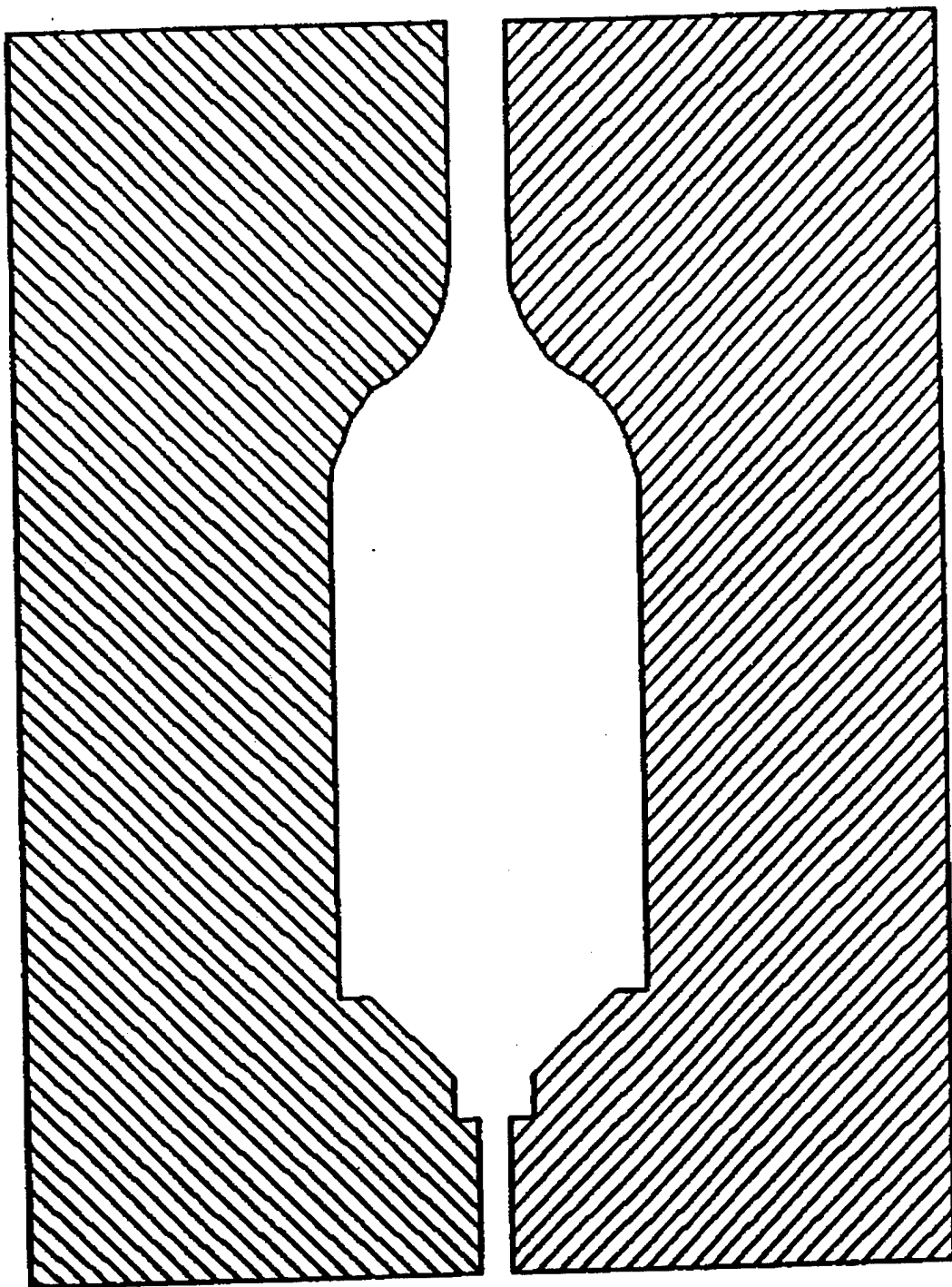


Figure 3. Sandia Test Fixture - Combustion Chamber.

corresponding to the first radial mode of the cylinder. This system is very similar to a liquid propellant rocket.

The numerical model is simplified as much as possible for this exercise. The chamber is assumed to be exactly a cylinder, ignoring the shape of the converging nozzle. The liquid is injected at a steady rate. The liquid instantaneously breaks up into droplets of a specified size and ignites. Combustion occurs according to a pressure-dependent burn rate, Ap^B . The liquid and gas have the same velocity and the same pressure at any point. Viscosity and turbulence are ignored. Heat transfer to the liquid is ignored. The liquid is assumed to be incompressible (treated as compressible in the code). The outflow is computed assuming choked flow. At all points within the fixture, the gas and liquid are assumed to move with the same velocity. The numerical simulations quickly reach pseudosteady state. The mean pressure and outflow rate are constant, but there are oscillations about the mean. For the dimensional analysis, the outflow rate is considered constant and equal to the inflow rate.

4.2 Eulerian Equations. In this section, the basic continuity, momentum, and energy equations are derived for the Sandia fixture. For mathematical simplicity, the equations are rendered in Cartesian coordinates. In actuality, the system is described best in cylindrical coordinates. The scaling relationships and insights are the same for both coordinate systems.

There are a large number of variables and parameters in the mathematical model for the Sandia fixture. All of these variables and parameters are defined in the List of Symbols. To facilitate the presentation, some of them are also defined in this section and in section 4.3.

The continuity equation for the gas is

$$\frac{\partial(\rho)}{\partial t} + \frac{\partial(\rho V_x)}{\partial x} + \frac{\partial(\rho V_y)}{\partial y} = S_{D \rightarrow G} = 4\pi\rho_L \dot{r}_D r_D^2 n. \quad (94)$$

The right-hand side of equation (94) is the volumetric increase in gas mass density by burning of the liquid drops.

Because the gas and droplets are assumed to move with the same velocity, we can use a volume average mass density for the gas plus droplets. This is defined by

$$\rho_T = \rho + \rho_D, \quad (95)$$

where ρ is the mass density of the gas (gas mass divided by volume) and ρ_D is the mass density of the droplets (liquid mass divided by volume).

The two momentum equations are

$$\frac{\partial(\rho_T V_x)}{\partial t} + \frac{\partial(\rho_T V_x^2)}{\partial x} + \frac{\partial(\rho_T V_y V_x)}{\partial y} = -\frac{\partial p}{\partial x} \quad (96)$$

and

$$\frac{\partial(\rho_T V_y)}{\partial t} + \frac{\partial(\rho_T V_x V_y)}{\partial x} + \frac{\partial(\rho_T V_y^2)}{\partial y} = -\frac{\partial p}{\partial y}. \quad (97)$$

The energy equation for the gas is

$$\frac{\partial}{\partial t} \left(\frac{1}{2} \rho V^2 + \rho u \right) + \nabla \cdot \left(\rho \vec{V} \left(\frac{1}{2} V^2 + h \right) \right) = e_L S_{D \rightarrow G}, \quad (98)$$

where

$$u = C_m T = \text{internal energy per unit mass}, \quad (99)$$

$$h = u + \frac{p}{\rho} = \text{enthalpy per unit mass}, \quad (100)$$

and

$$V^2 = V_x^2 + V_y^2. \quad (101)$$

The pressure is related to the density and temperature via the equation of state,

$$p = \frac{\rho_G RT}{1 - b\rho_G}, \quad (102a)$$

where ρ_G is the true gas density. It is given by

$$\rho_G = \frac{\rho}{1 - \frac{4\pi}{3}nr_D^3}, \quad (102b)$$

where n is the number density of the liquid drops.

We now consider the droplet dynamics. Because equations (95) to (98) describe the gas-plus-droplet system, there is no additional momentum equation for the droplets. We assume that heat transfer between droplets and gas is neglected and that droplets supply energy to the gas when they convert to gas. These assumptions preclude the need for an energy balance for the droplets. The only relevant equation for the droplets is the mass balance equation. This equation is given by

$$\frac{\partial(\rho_D)}{\partial t} + \frac{\partial(\rho_D V_x)}{\partial x} + \frac{\partial(\rho_D V_y)}{\partial y} = -S_{D \rightarrow G} = -4\pi\rho_L \dot{r}_D r_D^2 n, \quad (103)$$

where

$$\rho_D = n\rho_L v_D = n\rho_L \frac{4\pi}{3} r_D^3 \quad (104)$$

and

$$\dot{r}_D = Ap^B. \quad (105)$$

Dividing both sides of equation (103) by ρ_L and using equation (105) gives

$$\frac{\partial(nr_D^3)}{\partial t} + \frac{\partial(nr_D^3 V_x)}{\partial x} + \frac{\partial(nr_D^3 V_y)}{\partial y} = -3Ap^B r_D^2 n. \quad (106)$$

Equation (106) is a partial differential equation in two dependent variables: n and r_D . This, however, can be reduced to a single partial differential equation in the single variable, r_D , by recognizing that the continuity equation for the number density is

$$\frac{\partial(n)}{\partial t} + \frac{\partial(nV_x)}{\partial x} + \frac{\partial(nV_y)}{\partial y} = 0. \quad (107)$$

That is to say, even though the mass of a droplet is always decreasing, the droplet always exists—even though, in the limiting case, it may have zero mass. Differentiating the left-hand side of equation (106) and using equation (107) gives the following Eulerian description of the droplet radius:

$$\frac{\partial(r_D)}{\partial t} + V_x \frac{\partial(r_D)}{\partial x} + V_y \frac{\partial(r_D)}{\partial y} = -Ap^B. \quad (108)$$

Equation (108) applies only for $r_D \geq 0$.

In summary, we have a set of eight unknowns, ρ , ρ_T , V_x , V_y , p , T , n , and r_D , in eight equations, (94)–(98), (102), (107), and (108). The object now is to reduce this system of equations to an equivalent set of dimensionless equations that can be analyzed using a relatively small number of parameters.

4.3 Self-Similar Eulerian Equations. In this section, we convert the equations of the previous section to dimensionless forms. We define the following set of dimensionless variables:

$$\bar{\rho} = \rho / \rho_0, \bar{p} = p / p_0, \bar{T} = T / T_0, \bar{n} = n / n_0, \bar{r}_D = r_D / r_{D0}, \bar{V}_x = V_x / V_0, \text{ and } \bar{V}_y = V_y / V_0,$$

where the baseline values are denoted by the subscript 0. There is no restriction on the baseline values. When the foregoing dimensionless variables are inserted into the system of equations of section 4.2, we obtain a set of dimensionless equations. The dimensionless continuity equation is

$$\frac{\partial \bar{\rho}}{\partial \tau} + P_0 \frac{\partial (\bar{\rho} \bar{V}_x)}{\partial \bar{x}} + P_0 \frac{\partial (\bar{\rho} \bar{V}_y)}{\partial \bar{y}} = E_0 \bar{n} \bar{p}^B \bar{r}_D^2, \quad (109)$$

where

$$\bar{x} = \frac{x}{L} \text{ and } \bar{y} = \frac{y}{L}, \quad (110)$$

$$P_0 = \frac{V_0 T_{D0}}{L} = \frac{V_0 r_{D0}}{L A p_0^B}, \quad (111)$$

$$E_0 = \frac{4\pi \rho_L n_0 r_{D0}^3}{\rho_0}, \quad (112)$$

$$T_{D0} = \frac{r_{D0}}{Ap_0^B}, \quad (113)$$

and

$$\tau = \frac{t}{T_{D0}}. \quad (114)$$

The dimensionless momentum equations are

$$\frac{\partial(\bar{\rho}_T \bar{V}_x)}{\partial \tau} + P_0 \frac{\partial(\bar{\rho}_T \bar{V}_x^2)}{\partial \bar{x}} + P_0 \frac{\partial(\bar{\rho}_T \bar{V}_y \bar{V}_x)}{\partial \bar{y}} = -P_0 K_0 \frac{\partial \bar{p}}{\partial \bar{x}} \quad (115)$$

and

$$\frac{\partial(\bar{\rho}_T \bar{V}_y)}{\partial \tau} + P_0 \frac{\partial(\bar{\rho}_T \bar{V}_x \bar{V}_y)}{\partial \bar{x}} + P_0 \frac{\partial(\bar{\rho}_T \bar{V}_y^2)}{\partial \bar{y}} = -P_0 K_0 \frac{\partial \bar{p}}{\partial \bar{y}}, \quad (116)$$

where

$$K_0 = \frac{P_0}{\rho_0 V_0^2} \quad (117)$$

and

$$\bar{\rho}_T = (\bar{p} + \frac{E_0}{3} n \bar{r}_D^3). \quad (118)$$

The dimensionless energy equation becomes

$$\frac{\partial}{\partial \tau} \left(\frac{1}{2} \bar{\rho} \bar{V}^2 + \frac{\bar{\rho} C_m \bar{T} T_0}{V_0^2} \right) + P_0 \bar{\nabla} \cdot \left(\bar{\rho} \bar{\nabla} \left(\frac{1}{2} \bar{V}^2 + \frac{C_m \bar{T} T_0}{V_0^2} \right) \right) + K_0 P_0 \bar{\nabla} \cdot (\bar{\rho} \bar{\nabla}) = H_0 \bar{n} \bar{p}^B \bar{r}_D^2, \quad (119)$$

where

$$\bar{\nabla} = \bar{i} \frac{\partial}{\partial \bar{x}} + \bar{j} \frac{\partial}{\partial \bar{y}}, \quad (120)$$

$$H_0 = \frac{e_L}{V_0^2} E_0, \quad (121)$$

and

$$\bar{p} = \frac{\bar{\rho} \bar{T}}{1 - \bar{n} \bar{r}_D^3 \left(\frac{\rho_0}{3\rho_L} \right) - b\rho_0 \bar{\rho}} \left(\frac{\rho_0 T_0 R}{P_0} \right). \quad (122)$$

The dimensionless droplet equations are

$$\frac{\partial(\bar{n})}{\partial \tau} + P_0 \frac{\partial(\bar{n} \bar{V}_x)}{\partial \bar{x}} + P_0 \frac{\partial(\bar{n} \bar{V}_y)}{\partial \bar{y}} = 0 \quad (123)$$

and

$$\frac{\partial(\bar{r}_D)}{\partial \tau} + P_0 \bar{V}_x \frac{\partial(\bar{r}_D)}{\partial \bar{x}} + P_0 \bar{V}_y \frac{\partial(\bar{r}_D)}{\partial \bar{y}} = -\bar{p}^B. \quad (124)$$

Simplification of the dimensionless equations occurs by making the appropriate selections for the baseline parameters. This is where physical insight into the problem is of great value. There is a temptation to select values of pressure, temperature, and density at their initial values.

However, we know from experience that within a broad range of initial conditions, the response of liquid rocket systems and RLPG designs are essentially independent of the initial values of pressure, temperature, and density. Under these conditions, we are liberty to select p_0 , T_0 , and ρ_0 to simplify the dimensionless equations.

We select p_0 and ρ_0 to make $P_0 = 1$ and $E_0 = 1$. This gives

$$p_0 = \left(\frac{V_0 r_{D0}}{LA} \right)^{1/B}, \quad (125)$$

$$\rho_0 = 3\rho_L n_0 v_{D0}, \quad (126)$$

$$K_0 = \frac{p_0}{\rho_0 V_0^2} = \frac{(V_0 r_{D0})^{1/B}}{3(LA)^{1/B} \rho_L n_0 v_{D0}} = \frac{(V_0 r_{D0})^{1/B}}{3(LA)^{1/B} \rho_L \eta_{D0}}, \quad (127)$$

and

$$\eta_{D0} = n_0 v_{D0} = n_0 \frac{4\pi}{3} r_{D0}^3. \quad (128)$$

When the foregoing definitions are used, the dimensionless time now becomes

$$\tau = \frac{t}{T_{D0}}. \quad (129)$$

T_{D0} is now given by

$$T_{D0} = \frac{r_{D0}}{A p_0^B} = \frac{L}{V_0}. \quad (130)$$

The baseline temperature, T_0 , is selected to satisfy the condition

$$\frac{C_m T_0}{V_0^2} = 1. \quad (131)$$

This gives

$$T_0 = \frac{V_0^2}{C_m}. \quad (132)$$

When the foregoing definitions are used, the dimensionless time now becomes

$$\tau = \frac{t}{T_{D0}}, \quad (133)$$

where

$$T_{D0} = \frac{r_{D0}}{Ap_0^B} = \frac{L}{V_0}. \quad (134)$$

The new system of dimensionless equations now becomes

$$\frac{\partial \bar{p}}{\partial \tau} + \frac{\partial (\bar{\rho} \bar{V}_x)}{\partial \bar{x}} + \frac{\partial (\bar{\rho} \bar{V}_y)}{\partial \bar{y}} = \bar{n} \bar{p}^B \bar{r}_D^2, \quad (135)$$

$$\frac{\partial (\bar{\rho}_T \bar{V}_x)}{\partial \tau} + \frac{\partial (\bar{\rho}_T \bar{V}_x^2)}{\partial \bar{x}} + \frac{\partial (\bar{\rho}_T \bar{V}_y \bar{V}_x)}{\partial \bar{y}} = -K_0 \frac{\partial \bar{p}}{\partial \bar{x}}, \quad (136)$$

$$\frac{\partial(\bar{\rho}_T \bar{V}_Y)}{\partial \tau} + \frac{\partial(\bar{\rho}_T \bar{V}_X \bar{V}_Y)}{\partial \bar{x}} + \frac{\partial(\bar{\rho}_T \bar{V}_Y^2)}{\partial \bar{y}} = -K_0 \frac{\partial \bar{p}}{\partial \bar{y}}, \quad (137)$$

$$\bar{\rho}_T = \left(\bar{\rho} + \frac{E_0}{3} \bar{n} \bar{r}_D^3 \right), \quad (138)$$

$$\frac{\partial}{\partial \tau} \left(\bar{\rho} \left(\frac{1}{2} \bar{V}^2 + \bar{T} \right) \right) + \bar{\nabla} \cdot \left(\bar{\rho} \bar{\vec{V}} \left(\frac{1}{2} \bar{V}^2 + \bar{T} \right) \right) + K_0 \bar{\nabla} \cdot (\bar{p} \bar{\vec{V}}) = H_0 \bar{n} \bar{p}^B \bar{r}_D^2, \quad (139)$$

$$\bar{p} = \frac{\bar{\rho} \bar{T}}{1 - \bar{n} \bar{r}_D^3 \left(\frac{\rho_0}{3\rho_L} \right) - b\rho_0 \bar{\rho}} \left(\frac{\rho_0 T_0 R}{p_0} \right), \quad (140)$$

$$\frac{\partial(\bar{n})}{\partial \tau} + \frac{\partial(\bar{n} \bar{V}_X)}{\partial \bar{x}} + \frac{\partial(\bar{n} \bar{V}_Y)}{\partial \bar{y}} = 0, \quad (141)$$

and

$$\frac{\partial(\bar{r}_D)}{\partial \tau} + \bar{V}_X \frac{\partial(\bar{r}_D)}{\partial \bar{x}} + \bar{V}_Y \frac{\partial(\bar{r}_D)}{\partial \bar{y}} = -\bar{p}^B. \quad (142)$$

By writing equation (140) in the form

$$\bar{p} = \frac{\bar{\rho} \bar{T} \Omega_0}{1 - \bar{n} \bar{r}_D^3 \eta_{D0} - N_0 \bar{\rho}}, \quad (143)$$

where

$$N_0 = b\rho_0 = 3b\rho_L \eta_{D0} \quad (144)$$

and

$$\Omega_0 = \left(\frac{\rho_0 T_0 R}{p_0} \right) = \left(\frac{LA}{V_0 r_{D0}} \right)^{1/B} \left(\frac{3\rho_L \eta_{D0} V_0^2 R}{C_m} \right), \quad (145)$$

we arrive at a system of eight equations, (135) to (142); eight dimensionless variables, $\bar{\rho}$, $\bar{\rho}_T$, \bar{V}_x , \bar{V}_y , \bar{p} , \bar{T} , \bar{n} , and \bar{r}_D ; and five dimensionless constant parameters, K_0 , H_0 , η_{D0} , N_0 , and Ω_0 . Examination of η_{D0} and N_0 shows that we can eliminate one of these two since the covolume, b , is a constant and the liquid density is nearly constant. We keep η_{D0} and eliminate N_0 .

The solution for each of the variables (we use pressure as an example) can be expressed in the form

$$p = p_0 f_p \left(\frac{x}{L}, \frac{y}{L}, \tau, K_0, H_0, \eta_{D0}, \Omega_0 \right), \quad (146)$$

where

$$p_0 = \left(\frac{V_0 r_{D0}}{LA} \right)^{1/B} \quad (147)$$

and f_p is a function determined from the solution of equations (135) to (142). A different f function applies to each of the eight variables.

4.4 Confirmation of Scaling Relationships. Systems that have the same values of the dimensionless constant parameters K_0 , H_0 , η_0 , and Ω_0 will have similar time and space behavior when expressed in dimensionless variables. Consistency between the current Eulerian formulation and the Lagrangian formulation used in the code allows the examination of pressure oscillations to be made in the relatively limited dimensional space of only four parameters.

While the dimension space of the problem has been reduced, the relationships between the variables are still extremely complicated. However, analysis of the results indicates an interesting scaling relation. Suppose the dimensions of the chamber (radius, length, radius of inlet, radius of outlet) are increased by a constant factor. If either the radius of the injected droplets is increased by the factor or the pre-exponential term, A , is decreased by the factor, the normalizing factor, p_0 , is unchanged. The nondimensional time, τ , includes the constant, L , so the time scale will decrease by this factor. The other nondimensional quantities in the function, f_p , are unchanged. The injection velocity is left unchanged, so the mass flow increase is proportional to the vent area increase. The pressure should be the same, except for the change in the time scale.

This scaling law for the pressure seems reasonable physically. If the dimensions are increased, pressure waves will take longer to reach the walls of the chamber and return to the combustion site near the injector. If the combustion rate is decreased proportionally, the pressure waves will receive the same amount of energy at each iteration.

To check this result, numerical simulations were performed using the 2-D RLPG code. The baseline simulation for this fixture assumes the jet breaks up into 200- μm -diameter droplets. A pressure trace from the simulation at the top wall is shown in Figure 4. Very large oscillations are generated. The Fourier transform is shown in Figure 5. The largest frequency is a first radial mode (around 26 kHz). With the chamber represented as a cylinder (ignoring the actual nozzle shape at the exit) there is a first longitudinal mode (around 10 kHz). There are also smaller overtones.

Simulation was performed again with all the physical dimensions doubled. The size of the injected droplets is also doubled. The pressure at the middle of the top wall is shown in Figure 6. Note that the time scale has been changed. The Fourier transform is shown in Figure 5. The magnitudes are almost the same as the baseline case, while the frequencies are cut in half. In Figure 7, the frequencies of the doubled case are cut in half. There is no noticeable difference from the baseline case when the time scaled is thus adjusted. The same answer is obtained if the

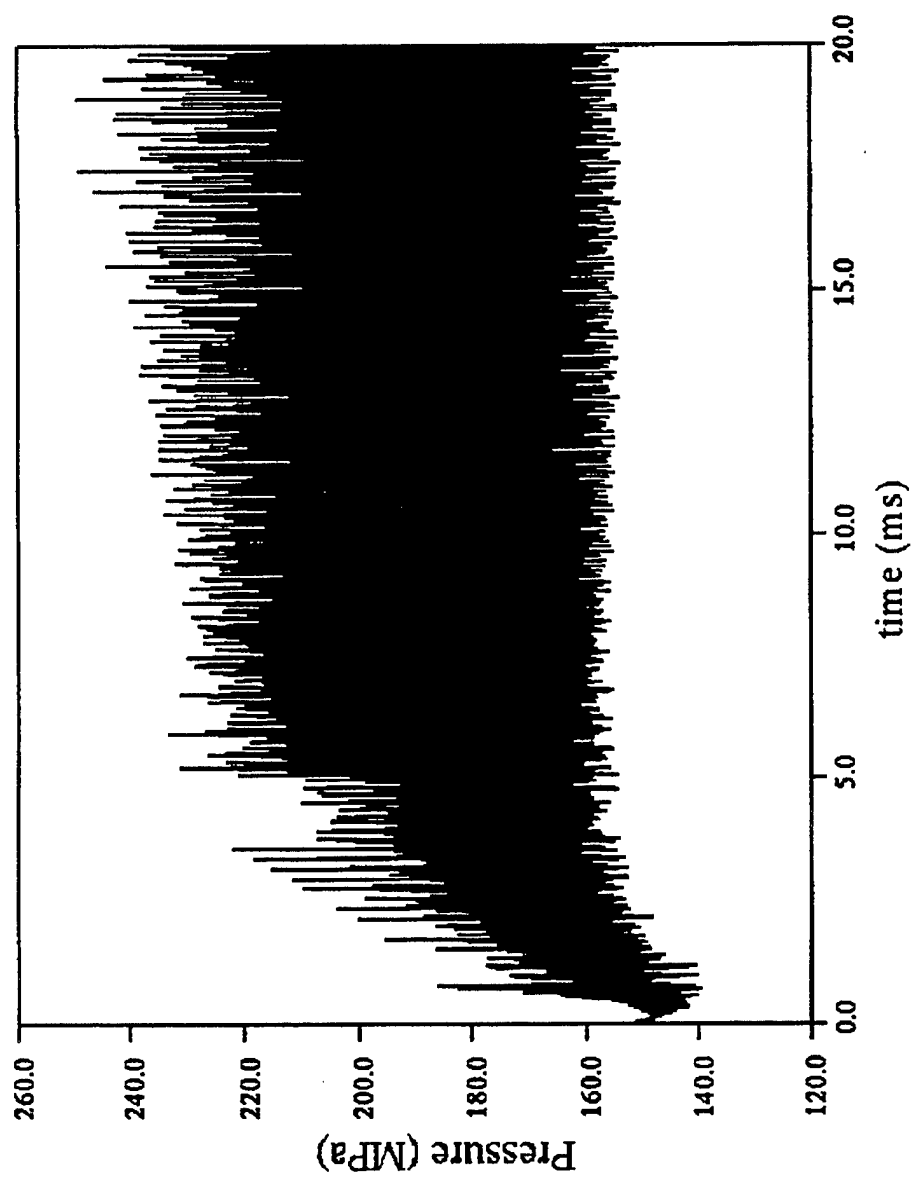


Figure 4. Sandia Test Fixture - Baseline: Simulation With 200- μ m-Diameter Droplets.

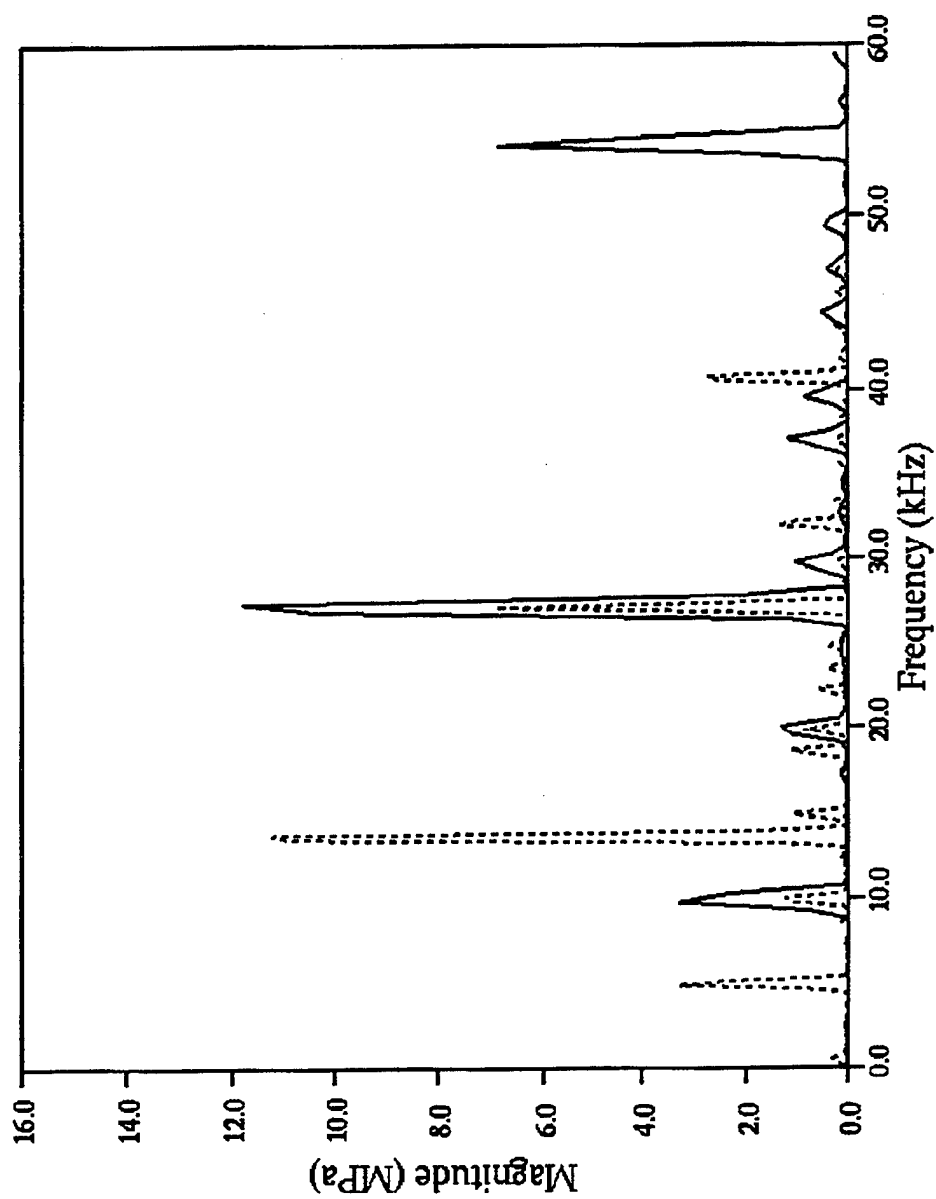


Figure 5. Baseline FFT (Line) and All Physical Dimensions Doubled FFT (Dot).

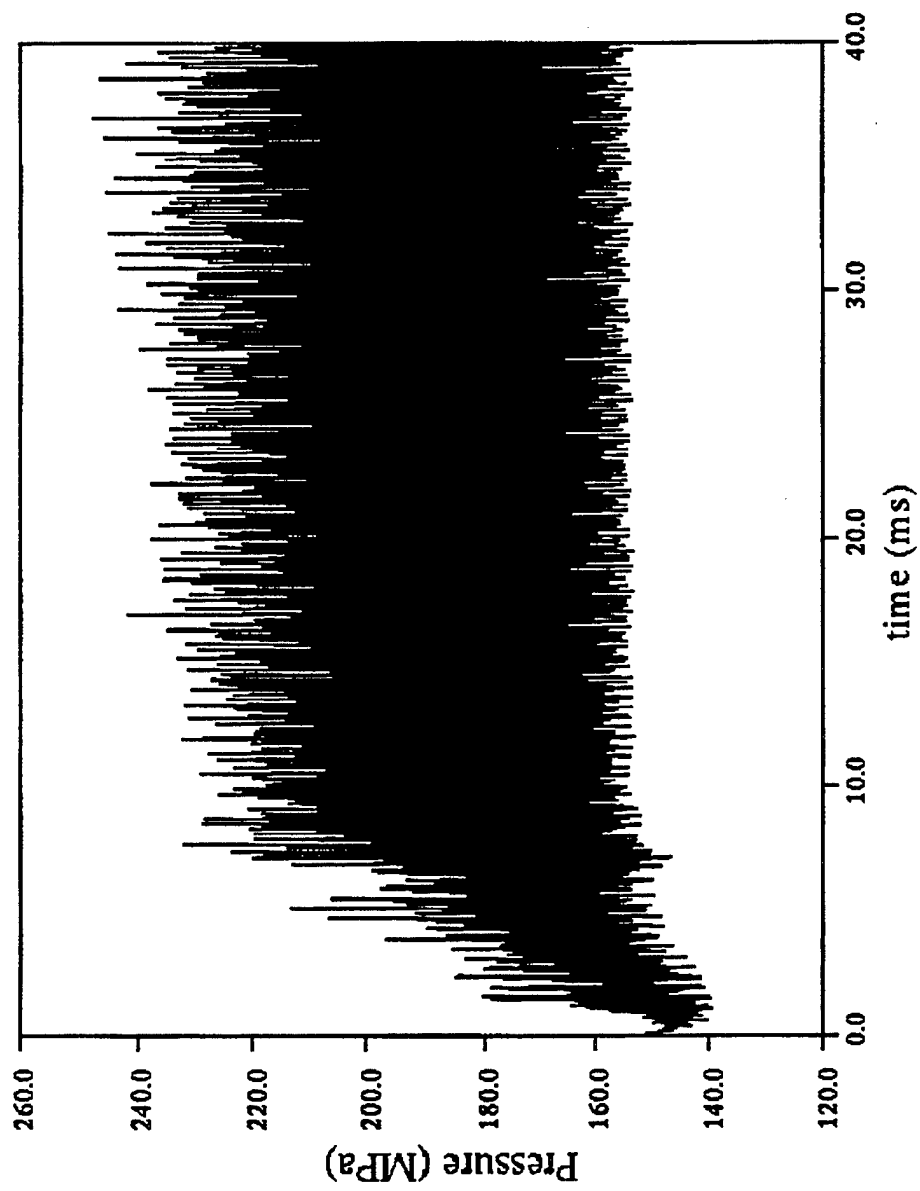


Figure 6. Sandia Test Fixture - Simulation With Dimensions Doubled: 400- μ m-Diameter Droplets.

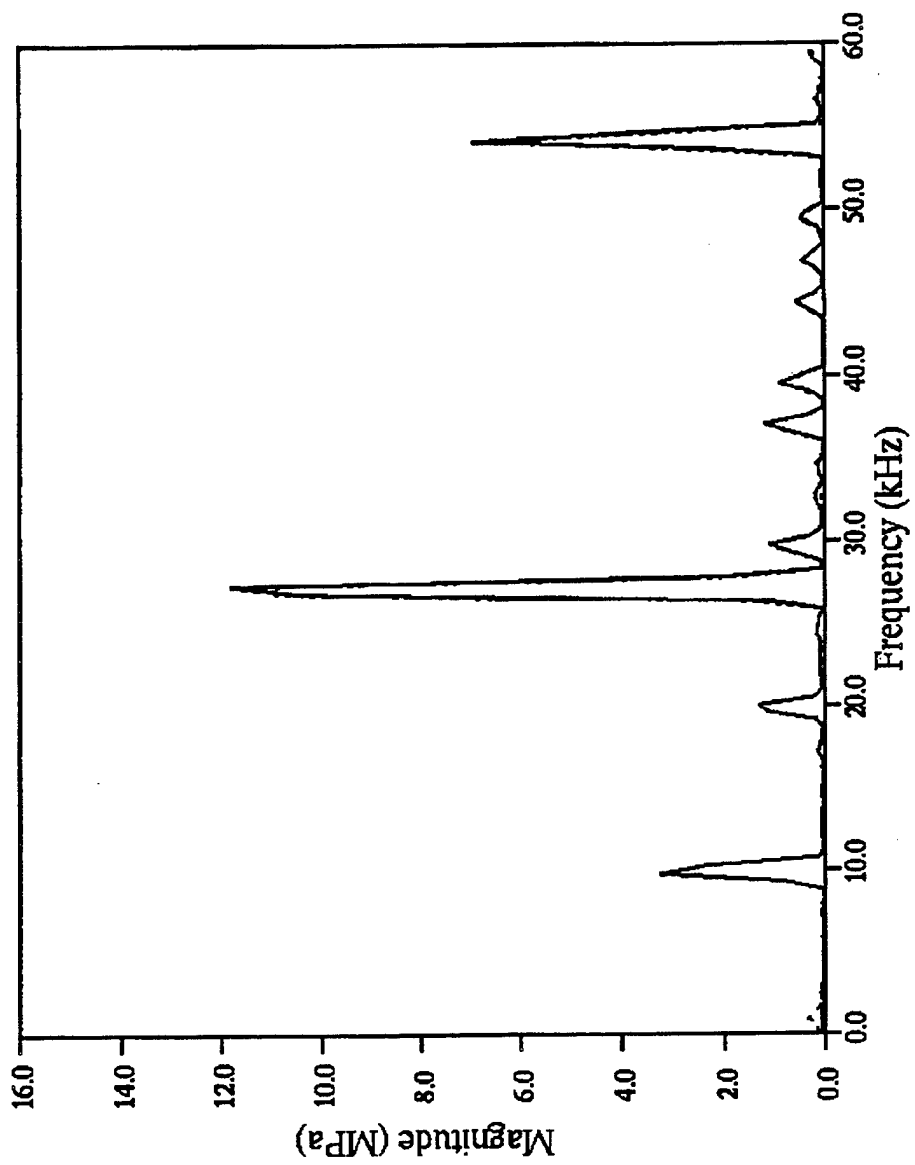


Figure 7. Baseline-FFT (Line) and Doubled-FFT Frequency Times 2 (Dot).

pre-exponential is cut in half and the droplet diameter is left at 200 μm . The model produces almost exactly the answer predicted by the dimensional analysis.

This result only holds if all the conditions are applied. For instance, suppose all the dimensions are doubled except for the length, which is left the same. The longitudinal mode, as expected, has a different frequency. But the radial mode is also very different in amplitude. Also, if the dimensions are doubled but the droplet diameter is left at 200 μm , a completely different answer is computed.

Standard correlations for injected droplet size show that the size depends primarily on the injection velocity and the ratio of the gas-to-liquid density [5]. So, if a scale up of the test fixture were constructed, we would expect that the injected droplet diameter would be about the same. This implies that, to actually construct a scale of a fixture that has the same magnitude of pressure oscillations as the original fixture, either the droplet diameter must be controlled or the burning rate of the propellant must be modified.

5. RLPG Considerations

The dimensionless equations for a gun simulation have not yet been derived. The problem is essentially transient and much more complicated than the aforementioned test fixture. However, based on physical intuition, some simulations were made to check whether the scaling rule still holds for gun conditions.

Figure 8 shows the pressure at the middle of the top wall of the chamber for a 30-mm gun simulation. The injected droplet diameter is now a function of time rather than a constant. The dimensions were then doubled (60-mm gun), and the injected droplet diameter profile was also doubled. Figure 9 shows the result. Again, note the different time scale. The curves are very similar. The Fourier transforms are almost the same for any time window during the firing cycle.

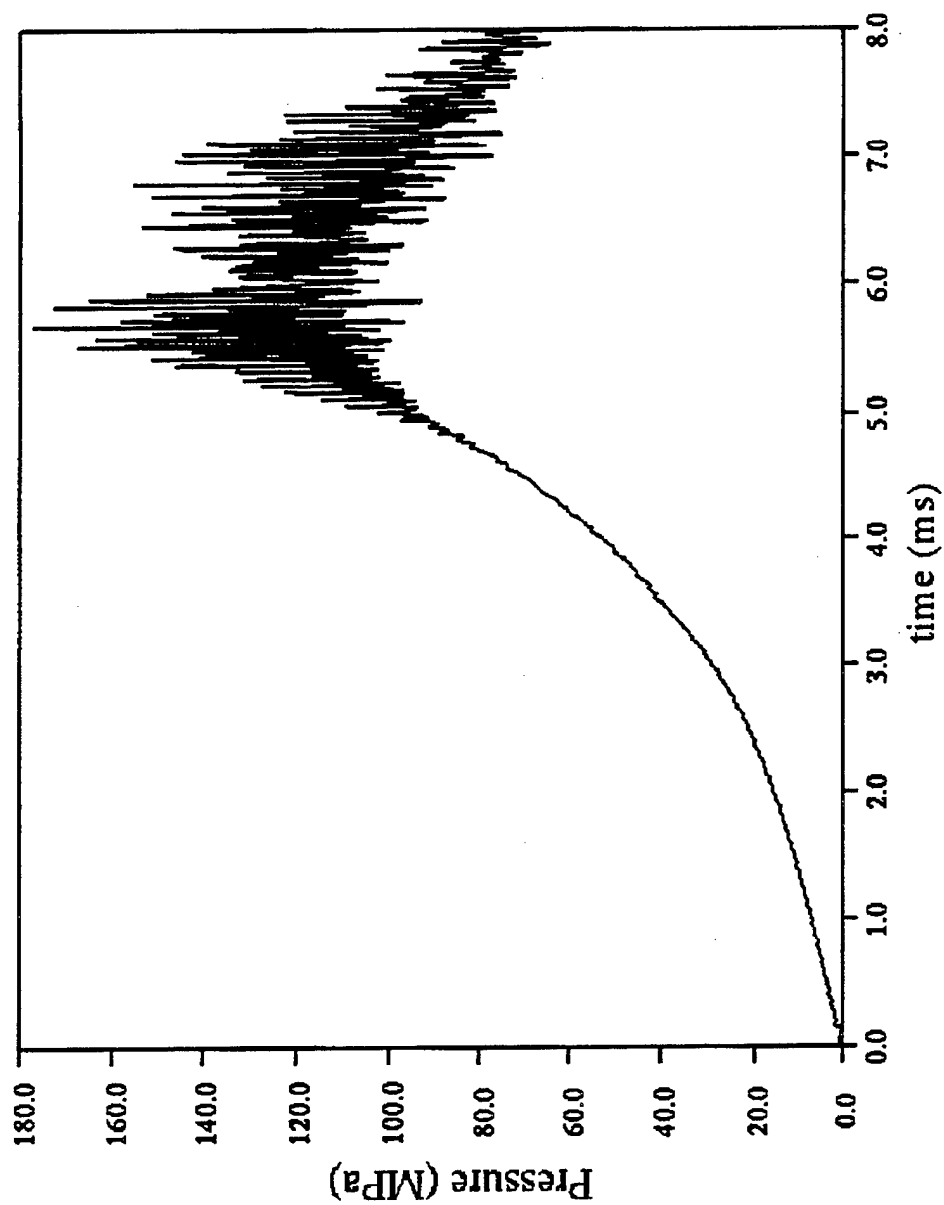


Figure 8. 30-mm Simulation - Pressure at Top Middle Wall.

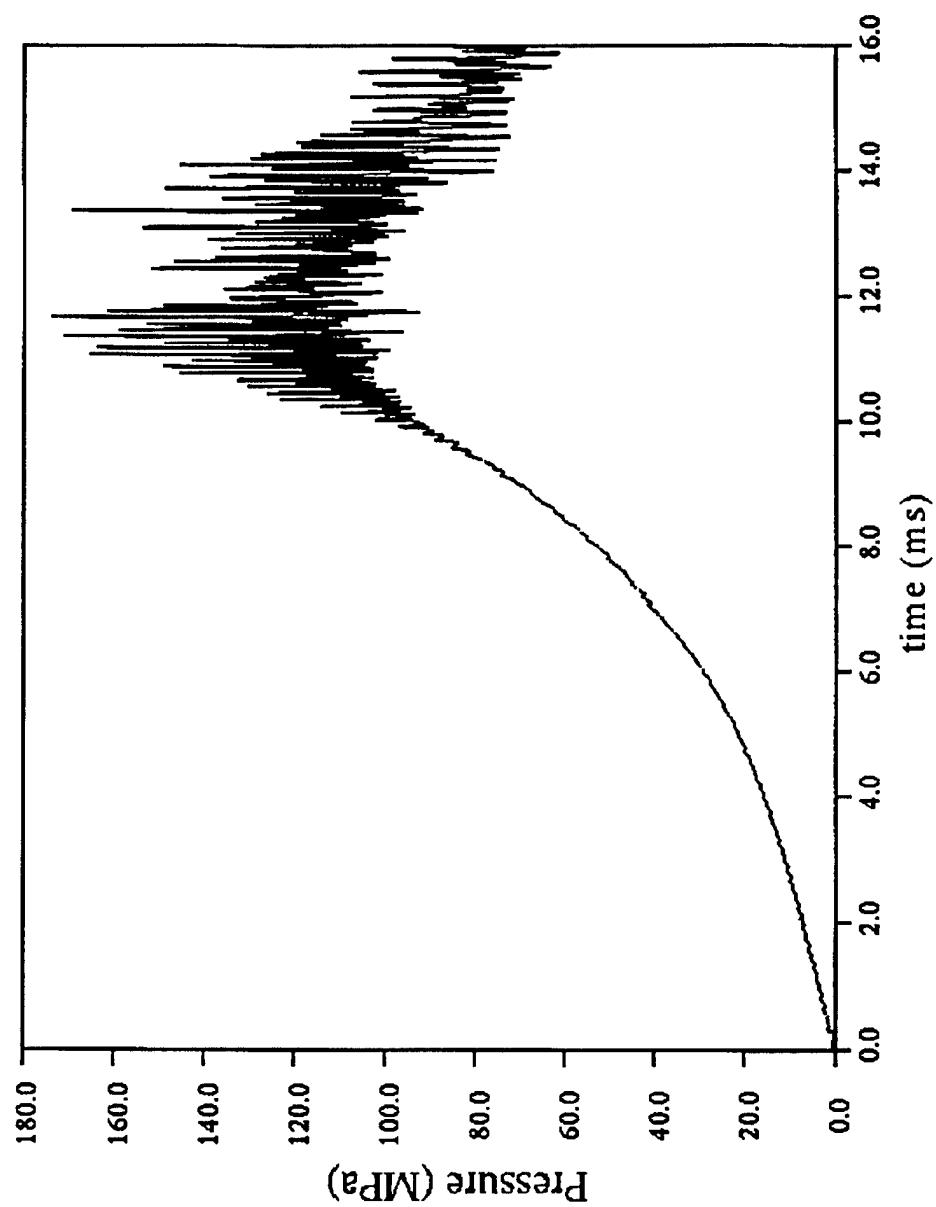


Figure 9. 60-mm Simulation - Pressure at Top Middle Wall.

6. Intact-Core Model

So far, all the simulations shown have assumed that the injected liquid instantaneously breaks up into droplets. This is a simplification of a much more complicated process. A number of other jet breakup models have also been considered [16]. The most useful has been to assume that most of the liquid is in a noncombusting intact core. Droplets stripped off the core are small, on the order of 10 μm . The length of the intact core depends on the ratio of the gas-to-liquid density and the diameter of the injector. So, the intact-core length should scale with the size of the fixture.

A number of simulations were performed using the intact-core model. Consider a 30-mm gun simulation. The length of the intact core and the size of the small combusting droplets outside the core vary through the firing cycle. This case was then scaled up to a 60-mm gun. If the length of the intact core and the size of the drops outside the core are doubled, the scaling law still holds. The pressure oscillations are the same magnitude, with the time scale doubled. However, if the small drops are kept the same size as in the 30-mm simulation, the solution is very different in character. It was expected that, once the droplets became small, the exact size would not be important. This turned out not to be the case. Thus, the scaling law for the intact-core model is essentially the same as for the droplet model.

7. Conclusion

Dimensional analysis has been applied to the equations governing RLPGs. A scaling law that relates fixtures of different sizes has been derived. The numerical model agrees almost exactly with the scaling law. This increases our confidence both in the dimensional analysis and the numerical accuracy of the computational fluid dynamics code.

It is useful to be able to do experiments in a smaller scale fixture. Unfortunately, the scaling rule derived here indicates that either the injected droplet size or the burn rate also has to be modified. The droplet size is not under our control for practical gun injectors, and the droplet

size is expected to be about the same for fixtures that operate at similar pressures. There has been some work in developing propellant with a faster burn rate [17]. However, the burn rate cannot be controlled with any precision.

It has long been noticed that pressure oscillations in 155-mm guns are very different in character than oscillations in 30-mm guns. Even when the same modes occur, the magnitudes are different. The present work indicates that this should, in fact, be expected. While we can scale the physical dimensions of the 30-mm gun, we cannot control the droplet size or the burn rate of the propellant.

INTENTIONALLY LEFT BLANK.

8. References

1. Wren, G., T. P. Coffee, and J. Knapton. "Pressure Oscillations in RLPGs." *Journal of Propellants, Explosives, and Pyrotechnics*, vol. 20, no. 1, pp. 225-231, 1995.
2. Klingsberg, G., J. Knapton, W. Morrison, and G. Wren. "Liquid Propellant Gun Technology." *Progress in Astronautics and Aeronautics*, vol. 175, Reston, VA, 1997.
3. Coffee, T. P. "A Lumped Parameter Code for Regenerative Liquid Propellant Guns." BRL-TR-2703, U.S. Army Ballistic Research Laboratory, Aberdeen Proving Ground, MD, December 1985.
4. Coffee, T. P. "An Updated Lumped Parameter Code for Regenerative Liquid Propellant In-Line Guns." BRL-TR-2974, U.S. Army Ballistic Research Laboratory, Aberdeen Proving Ground, MD, December 1988.
5. Coffee, T. P., P. G. Baer, W. F. Morrison, and G. P. Wren. "Jet Breakup and Combustion Modeling for the Regenerative Liquid Propellant Gun." BRL-TR-3223, U.S. Army Ballistic Research Laboratory, Aberdeen Proving Ground, MD, April 1991.
6. Coffee, T. P., and G. P. Wren. "Analysis of Repeatability Data for the Second-Generation 155-mm Concept VIC Regenerative Liquid Propellant Gun (RLPG)." ARL-TR-1157, U.S. Army Research Laboratory, Aberdeen Proving Ground, MD, July 1996.
7. Wolfe, H. E., and W. H. Andersen. "Kinetics, Mechanism, and Resultant Droplet Sizes of the Aerodynamic Breakup of Liquid Drops." Aerojet Report No. 0395-04(18)SP, April 1964.
8. Coffee, T. P. "A Two-Dimensional Model for the Combustion Chamber/Gun Tube of a Concept VIC Regenerative Liquid Propellant Gun." BRL-TR-3341, U.S. Army Ballistic Research Laboratory, Aberdeen Proving Ground, MD, May 1992.
9. Coffee, T. P. "A Two-Dimensional Model for Pressure Oscillations: Extension to Generalized Geometry." ARL-TR-349, U.S. Army Research Laboratory, Aberdeen Proving Ground, MD, January 1994.
10. Buckingham, E. "On Physically Similar Systems; Illustrations of the Use of Dimensional Equations." *Physics Review*, vol. IV, no. 4, pp. 345, 1914.
11. Sedov, L. I. *Similarity and Dimensional Methods in Mechanics*. MIR Publishers, Moscow, Russia, 1982.

12. Birkhoff, G. *Hydrodynamics: A Study in Logic, Fact, and Similitude*. Princeton University Press, Princeton, NJ, 1960.
13. Streeter, V. L. *Fluid Mechanics*. 4th Edition, McGraw-Hill Book Company, New York, 1996.
14. Kohlberg, I., D. Brown, and W. Jeffrey. "Application of Similarity Techniques for Verification of RV Flow Field Models in the TMD Regime." *Proceeding of the 6th Annual AIAA/BMDO Technology Readiness Conference and Exhibit*, San Diego, CA, 18-22 August 1997.
15. Carling, R. W., R. E. Rychnovsky, and S. K. Griffiths. "A Liquid Propellant Injector/Combustor." *Proceedings of the JANNAF Propulsion Meeting*, Cleveland, OH, 23-25 May 1989.
16. Coffee, T. P. "Progress in Modeling Pressure Oscillations in 30-mm Regenerative Liquid Propellant Guns." ARL-TR-1582, U.S. Army Research Laboratory, Aberdeen Proving Ground, MD, January 1998.
17. Klein, N., T. P. Coffee, and C. S. Leveritt. "Pressure Oscillations in a Liquid Propellant Gun - Possible Dependence on Propellant Burn Rate." BRL-TR-3361, U.S. Army Ballistic Research Laboratory, Aberdeen Proving Ground, MD, June 1992.

List of Symbols

d.1	$\rho(\bar{r}, t)$	Instantaneous average gas density
d.2	ρ_0	Reference average gas density
d.3	$\bar{\rho} = \frac{\rho}{\rho_0}$	Dimensionless gas density
d.4	$\rho_G(\bar{r}, t) = \frac{\rho(\bar{r}, t)}{1 - \eta_D(\bar{r}, t)}$	Instantaneous true gas density
d.5	$\rho_{G0} = \frac{\rho_0}{1 - \eta_{D0}}$	Reference true gas density
d.6	$\eta_D = n(\bar{r}, t) v_D(\bar{r}, t)$	Instantaneous fraction of volume occupied by the liquid
d.7	$1 - \eta_D(\bar{r}, t)$	Instantaneous fraction of volume occupied by the gas
d.8	$\eta_{D0} = n_0 v_{D0}$	Reference fraction of volume occupied by the liquid
d.9	$1 - \eta_{D0}$	Reference fraction of volume occupied by the gas
d.10	$v_D(\bar{r}, t) = \frac{4\pi}{3} r_D^3(\bar{r}, t)$	Instantaneous volume of droplet
d.11	$r_D(\bar{r}, t)$	Instantaneous radius of droplets
d.12	$v_{D0} = \frac{4\pi}{3} r_{D0}^3$	Reference volume of droplet
d.13	r_{D0}	Reference radius of droplets entering system
d.14	$\bar{r}_D = \frac{r_D}{r_{D0}}$	Dimensionless ratio of droplet radii
d.15	$\bar{r}_{D0} = 1$	Reference value of dimensionless radius
d.16	$n(\bar{r}, t)$	Instantaneous number density of droplets
d.17	n_0	Reference number density of droplets
d.18	$\bar{n} = \frac{n}{n_0}$	Dimensionless ratio of droplet density
d.19	$\bar{n}_0 = 1$	Reference value of dimensionless droplet density
d.20	$m_D(\bar{r}, t) = \rho_L v_D(\bar{r}, t)$	Instantaneous mass of droplet
d.21	m_{D0}	Reference mass of droplet
d.22	\bar{m}_D	Dimensionless droplet mass

d.23	$\bar{m}_{D0} = 1$	Reference value of dimensionless mass
d.24	ρ_L	Mass density of liquid
d.25	$\rho_D = n m_D = n \rho_L v_D$	Instantaneous droplet mass density
d.26	$\rho_{D0} = n_0 \rho_L v_{D0}$	Reference droplet mass density
d.27	$\bar{\rho}_D$	Dimensionless droplet mass density
d.28	$\bar{\rho}_{D0} = 1$	Reference value of dimensionless droplet mass density
d.29	$p(\vec{r}, t)$	Instantaneous gas pressure
d.30	p_0	Reference gas pressure
d.31	$\bar{p} = \frac{p}{p_0}$	Dimensionless pressure ratio
d.32	b	Covolume
d.33	R	Universal gas constant
d.34	$T(\vec{r}, t)$	Instantaneous temperature
d.35	T_0	Reference temperature
d.36	$\bar{T} = \frac{T}{T_0}$	Dimensionless temperature
d.37	e_L	Chemical energy
d.38	$\dot{r}_D = A p^B$	Burning rate
d.39	C_m	Specific heat per unit mass for gas at constant volume
d.40	γ	Ratio of specific heats
d.41	$u(\vec{r}, t) = C_m T(\vec{r}, t)$	Internal energy per unit mass
d.42	$h(\vec{r}, t) = u(\vec{r}, t) + \frac{p}{\rho}$	Instantaneous average enthalpy per unit mass for gas
d.43	$p = \frac{\rho_G R T}{1 - b \rho_G}$	Equation of state for gas
d.44	$\vec{V}_G(\vec{r}, t) = \vec{i} V_{Gx} + \vec{j} V_{Gy}$	Velocity of gas
d.45	$\vec{V}_D(\vec{r}, t) = \vec{i} V_{Dx} + \vec{j} V_{Dy}$	Velocity of droplets
d.46	$\vec{V}_{D0} = \vec{i} V_0$	Reference velocity of droplets (entrance conditions)
d.47	$\bar{V}_x = \frac{V_{Gx}}{V_0} = \frac{V_{Dx}}{V_0}$	Dimensionless x-component of droplet and gas velocity

d.48	$\bar{V}_Y = \frac{V_{GY}}{V_0} = \frac{V_{DY}}{V_0}$	Dimensionless y-component of droplet and gas velocity
d.49	V_{XE}	Exit x-component velocity of gas
d.50	$V_{YE} = 0$	Exit y-component velocity of gas
d.51	$\bar{V}_{XE} = \frac{V_{XE}}{V_0}$	Dimensionless exit x-component of gas velocity
d.52	$\bar{V}_{YE} = \frac{V_{YE}}{V_0} = 0$	Dimensionless exit y-component of gas velocity
d.53	$T_{D0} = \frac{r_{D0}}{Ap_0^B}$	Droplet regression time constant
d.54	$c_0 = (RT_0)^{1/2}$	Sound velocity divided by $\sqrt{\gamma}$
d.55	α_0	bp_{G0}
d.56	β_0	$\frac{e_L}{C_m T_0}$
d.57	$\bar{x} = \frac{x}{L}$	Dimensionless length in x-direction
d.58	$\bar{y} = \frac{y}{L}$	Dimensionless length in y-direction
d.59	L	Characteristic length
d.60	$\tau = \frac{t}{T_{D0}}$	Dimensionless time
d.61	$P_0 = \frac{V_0 T_{D0}}{L} = f_0 T_{D0}$	Dimensionless parameter
d.62	$f_0 = \frac{V_0}{L}$	Frequency associated with reference velocity
d.63	$E_0 = \frac{3\rho_L \eta_{D0}}{\rho_0}$	Dimensionless parameter
d.64	$\bar{\rho}_T = (\bar{\rho} + \frac{E_0}{3} \bar{n} \bar{r}_D^3)$	Dimensionless combined gas-plus-droplet density
d.65	$K_0 = \frac{p_0}{\rho_0 V_0^2}$	Dimensionless parameter
d.66	$H_0 = \frac{e_L}{V_0^2} E_0$	Dimensionless parameter

INTENTIONALLY LEFT BLANK.

<u>NO. OF COPIES</u>	<u>ORGANIZATION</u>
2	DEFENSE TECHNICAL INFORMATION CENTER DTIC DDA 8725 JOHN J KINGMAN RD STE 0944 FT BELVOIR VA 22060-6218
1	HQDA DAMO FDQ D SCHMIDT 400 ARMY PENTAGON WASHINGTON DC 20310-0460
1	OSD OUSD(A&T)/ODDDR&E(R) R J TREW THE PENTAGON WASHINGTON DC 20301-7100
1	DPTY CG FOR RDA US ARMY MATERIEL CMD AMCRDA 5001 EISENHOWER AVE ALEXANDRIA VA 22333-0001
1	INST FOR ADVNCD TCHNLGY THE UNIV OF TEXAS AT AUSTIN PO BOX 202797 AUSTIN TX 78720-2797
1	DARPA B KASPAR 3701 N FAIRFAX DR ARLINGTON VA 22203-1714
1	NAVAL SURFACE WARFARE CTR CODE B07 J PENNELLA 17320 DAHLGREN RD BLDG 1470 RM 1101 DAHLGREN VA 22448-5100
1	US MILITARY ACADEMY MATH SCI CTR OF EXCELLENCE DEPT OF MATHEMATICAL SCI MADN MATH THAYER HALL WEST POINT NY 10996-1786

<u>NO. OF COPIES</u>	<u>ORGANIZATION</u>
1	DIRECTOR US ARMY RESEARCH LAB AMSRL DD 2800 POWDER MILL RD ADELPHI MD 20783-1197
1	DIRECTOR US ARMY RESEARCH LAB AMSRL CS AS (RECORDS MGMT) 2800 POWDER MILL RD ADELPHI MD 20783-1145
3	DIRECTOR US ARMY RESEARCH LAB AMSRL CI LL 2800 POWDER MILL RD ADELPHI MD 20783-1145
	<u>ABERDEEN PROVING GROUND</u>
4	DIR USARL AMSRL CI LP (BLDG 305)

NO. OF
COPIES ORGANIZATION

1	COMMANDER US ARMY ARDEC WECAC WEE D DOWNS BLDG 3022B PICATINNY ARSENAL NJ 07806-5000
1	COMMANDANT US ARMY ARMOR CTR ATSB CD MLD FT KNOX KY 40121
1	COMMANDANT USAFAS ATST TSM CN FT SILL OK 78503-5600
2	COMMANDER HQ AMCCOM AMSMC LSL B KELEBER AMSMC SAS WF G SCHELENKER ROCK ISLAND IL 61299-6000
1	US MILITARY ACADEMY DEPT CVL AND MECHL ENGRG COL J SAMPLES MAHAN HALL OFC 322 WEST POINT NY 10966
3	CRAFT TECH INC COMBSTN RSRCH AND FLOW TECHLGY S DASH A HOSANGADI N SINHA 174 NORTH MAIN ST BLDG 3 DUBLIN PA 18917
3	GEN DYNMCS DEFNS SYS T KURIATA I MAGOON G KEELER 100 PLASTICS AVE PITTSFIELD MA 01201-3698

NO. OF
COPIES ORGANIZATION

ABERDEEN PROVING GROUND

1	CDR TECOM AMSTE TC
1	DIR ERCED SCBRD-RT
1	CDR CBDCOM AMSCB-CII
26	DIR USARL AMSRL SL AMSRL WM B A HORST AMSRL WM BA J KNAPTON AMSRL WM BC P PLOSTINS AMSRL WM BD B FORCH AMSRL WM BE T COFFEE (5 CPS) G WREN (5 CPS) A BIRK J DESPIRITO C LEVERITT T MINOR W OBERLE K WHITE L-M CHANG J COLBURN P CONROY D KOOKER M NUSCA

REPORT DOCUMENTATION PAGE			Form Approved OMB No. 0704-0188	
<small>Public reporting burden for this collection of information is estimated to average 1 hour per response, including the time for reviewing instructions, searching existing data sources, gathering and maintaining the data needed, and completing and reviewing the collection of information. Send comments regarding this burden estimate or any other aspect of this collection of information, including suggestions for reducing this burden, to Washington Headquarters Services, Directorate for Information Operations and Reports, 1215 Jefferson Davis Highway, Suite 1204, Arlington, VA 22202-4302, and to the Office of Management and Budget, Paperwork Reduction Project (0704-0188), Washington, DC 20503.</small>				
1. AGENCY USE ONLY (Leave blank)		2. REPORT DATE January 2000		3. REPORT TYPE AND DATES COVERED Final, Jan 98 - Mar 99
4. TITLE AND SUBTITLE Dimensional Analysis and Self-Similarity Theory for Regenerative Liquid Propellant Guns			5. FUNDING NUMBERS 1L16261841FL	
6. AUTHOR(S) I. Kohlberg* and T. P. Coffee				
7. PERFORMING ORGANIZATION NAME(S) AND ADDRESS(ES) U.S. Army Research Laboratory ATTN: AMSRL-WM-BE Aberdeen Proving Ground, MD 21005-5066			8. PERFORMING ORGANIZATION REPORT NUMBER ARL-TR-2157	
9. SPONSORING/MONITORING AGENCY NAME(S) AND ADDRESS(ES)			10. SPONSORING/MONITORING AGENCY REPORT NUMBER	
11. SUPPLEMENTARY NOTES * Kohlberg Associates, Inc., 5375 Duke St., Unit 1603, Alexandria, VA 22304				
12a. DISTRIBUTION/AVAILABILITY STATEMENT Approved for public release; distribution is unlimited.			12b. DISTRIBUTION CODE	
13. ABSTRACT (Maximum 200 words) <p>Regenerative liquid propellant guns (RLPGs) have been studied for many years. RLPG firings almost always show large, high-frequency pressure oscillations. To study this phenomenon, a fluid dynamics model of the combustion chamber/gun tube of an RLPG has been developed. High-frequency oscillations are generated naturally by the physics modeled in the code. Dimensional analysis has been applied to the governing equations to furnish insight into the dynamic relationships among pressure, density, temperature, droplet size, etc. The dimensional analysis predicts a scaling law between different-sized fixtures. The computational results exactly match these predictions. This agreement establishes the basis of self-similarity in the physical processes (e.g., tradeoff between droplet size and burning rate) and, in addition, helps verify the computational model.</p>				
14. SUBJECT TERMS dimensional analysis, fluid dynamics, regenerative gun, pressure oscillations, two-dimensional model			15. NUMBER OF PAGES 72	
			16. PRICE CODE	
17. SECURITY CLASSIFICATION OF REPORT UNCLASSIFIED	18. SECURITY CLASSIFICATION OF THIS PAGE UNCLASSIFIED	19. SECURITY CLASSIFICATION OF ABSTRACT UNCLASSIFIED	20. LIMITATION OF ABSTRACT UL	

INTENTIONALLY LEFT BLANK.

USER EVALUATION SHEET/CHANGE OF ADDRESS

This Laboratory undertakes a continuing effort to improve the quality of the reports it publishes. Your comments/answers to the items/questions below will aid us in our efforts.

1. ARL Report Number/Author ARL-TR-2157 (Kohlberg [POC: T. Coffee]) Date of Report January 2000
2. Date Report Received _____
3. Does this report satisfy a need? (Comment on purpose, related project, or other area of interest for which the report will be used.) _____

4. Specifically, how is the report being used? (Information source, design data, procedure, source of ideas, etc.) _____

5. Has the information in this report led to any quantitative savings as far as man-hours or dollars saved, operating costs avoided, or efficiencies achieved, etc? If so, please elaborate. _____

6. General Comments. What do you think should be changed to improve future reports? (Indicate changes to organization, technical content, format, etc.) _____

CURRENT
ADDRESS

Organization

Name

E-mail Name

Street or P.O. Box No.

City, State, Zip Code

7. If indicating a Change of Address or Address Correction, please provide the Current or Correct address above and the Old or Incorrect address below.

OLD
ADDRESS

Organization

Name

Street or P.O. Box No.

City, State, Zip Code

(Remove this sheet, fold as indicated, tape closed, and mail.)
(DO NOT STAPLE)